



TECHNISCHE
UNIVERSITÄT
WIEN



MASTER THESIS

Design and implementation of a brake-by-wire system for e-scooters

carried out for the purpose of obtaining the degree of Diplom-Ingenieur (Dipl.-Ing)

submitted at TU Wien

Faculty of Mechanical and Industrial Engineering

by

Stefano Cavosi, BSc



under the supervision of

Senior Lecturer Dipl.-Ing. Dr.techn. Florian Klinger

Institute of Mechanics and Mechatronics

Research Unit of Technical Dynamics and Vehicle System Dynamics

E325-01

Vienna, April 2024

Affidavit

I declare in lieu of oath, that I wrote this thesis and carried out the associated research myself, using only the literature cited in this volume. If text passages from sources are used literally, they are marked as such.

I confirm that this work is original and has not been submitted for examination elsewhere, nor is it currently under consideration for a thesis elsewhere. I acknowledge that the submitted work will be checked electronically-technically using suitable and state-of-the-art means (plagiarism detection software). On the one hand, this ensures that the submitted work was prepared according to the high-quality standards within the applicable rules to ensure good scientific practice "Code of Conduct" at the TU Wien. On the other hand, a comparison with other student theses avoids violations of my personal copyright.

Vienna, April 2024

Stefano Cavosi, BSc

Acknowledgements

Zuerst möchte ich meinem Betreuer Senior Lecturer Dipl.-Ing. Dr.techn. Florian Klinger für seine kontinuierliche Unterstützung in den letzten sieben Monaten danken. Vielen Dank für all die Geduld und Zeit, die er sich genommen hat, um meine vielen Fragen zu beantworten. Trotz der vielen anderen laufenden Projekte war er immer verfügbar, um Unklarheiten zu klären und sicherzustellen, dass das Projekt erfolgreich innerhalb enger Zeitgrenzen abgeschlossen wird.

Ein Dank geht auch an Univ.Prof. Dipl.-Ing. Dr.techn. Johannes Edelmann und Ao.Univ.Prof. Dipl.-Ing. Dr.techn. Manfred Plöchl für ihre Tipps und Hilfe dank ihrer umfangreichen Erfahrung mit solchen Projekten.

Ein Dank geht an alle Kollegen, Professoren, Doktoranden und Diplomanden des Mechanik-Instituts im 5. Stock, die immer freundlich und hilfsbereit zu mir waren. Ein besonderer Dank geht an all meine Bürokollegen, die mich täglich unterstützt und ertragen haben. Vor allem danke ich Andreas, meinem Qualitätskontrolleur, der sich immer Zeit genommen hat, um jeden Aspekt meiner Konstruktionen zu überprüfen. Ein Dank geht auch an meine Projektkollegen Matthias, der mir am Anfang geholfen hat, mich im Projekt einzuleben, und Lorenz für seine unverzichtbare Unterstützung, besonders in den letzten Wochen, als er sich ohne Verpflichtung viel Zeit genommen hat, um sicherzustellen, dass mein Projekt auch elektronisch funktioniert. Infine grazie a Luca per la compagnia e il suo costante buonumore durante le pause pranzo, caffè e durante le sessioni serali di lavoro. Grazie, buona guarigione alla tua cavaglia e in bocca al lupo a Vienna!

Zu guter Letzt möchte ich meinen Werkstattkollegen Manfred, Reinhold und Christoph danken, die die Umsetzung und Fertigung der e-Scooter Komponenten in Rekordzeit ermöglicht haben. Danke an Manfred für die ausgezeichneten doppelten Espresso, an Reinhold für seine ständige Verfügbarkeit und Unterstützung und an Christoph für seine Freundlichkeit und die schönen und lehrreichen Momente in der Werkstatt.

Danke auch an meine Freunde und Studienkollegen in Wien. Danke an all meine Studienkollegen, aber vor allem an Georg, der immer so freundlich mit mir war und die Geduld hatte, auf mich zu warten und mir unzählige Male alles zu erklären, was ich nicht verstand. Danke an meine Freunde vom 22. Bezirk, mit denen es immer eine Freude war, sich zu treffen, um dem Universitätsleben zu entfliehen, und danke an Basti, der ein fantastischer Freund ist, freundlich, fürsorglich und hilfsbereit.

Thanks also to all the friends and colleagues I made during my Erasmus experience in Gothenburg; they were an integral part of making it an amazing journey, both personally and academically.

Ich kann meine Mitbewohner, Freunde und Kollegen Theresia und Micha nicht genug

danken. Euch (wortwörtlich) vom ersten bis zum letzten Tag an meiner Seite zu haben, war eines der schönsten Geschenke, die ich bekommen konnte.

Ein ganz besonderer Dank geht natürlich an Micha, Studienkollege, Mitbewohner, Freund und Bruder fürs Leben. Danke für das Kochen, die Läufe, die Radtouren, die Ausflüge, die Pizzen, die Partys, die Abende, an denen wir Brettspiele gespielt oder einfach nur über alles geplaudert haben. Es waren intensive Jahre mit glücklichen und auch vielen schwierigen Momenten, aber wir haben sie alle geteilt. Du bist eine wunderbare Person, und ich bin glücklich, dich an meiner Seite zu haben. Ich habe viel von deiner Resilienz, deiner Neugierde und deiner Art, die Dinge zu sehen, gelernt. Danke für alles.

Ein besonderer Dank geht auch an meine Gastfamilie, Renate, Adi und Thomas, auch wenn wir uns nicht allzu oft sehen, weiß ich, dass ihr für mich da seid, egal was passiert.

Un grazie alla mia famiglia, a papà Roberto, mamma Margherita e sorella Elena, che mi hanno supportato fino a questo traguardo. Grazie mille di tutto quello che mi avete insegnato, soprattutto la resilienza in situazioni difficili e la passione in ciò che si fa. Grazie di aver reso possibile tutto questo. Grazie alla mamma Margherita per il suo costante supporto morale e pratico con le sue scorte di cibo, grazie a papà Roberto per i suoi saggi consigli e il suo supporto in tutte le mie decisioni. Grazie anche per tutti i passaggi in macchina a orari scomodissimi a Bolzano e a Innsbruck, saper di poter contare su di voi è sempre stato un aiuto enorme. Grazie alla mia sorellina Elenina che nonostante gli sporadici bisticci mi vuole bene e mi supporta sempre. Grazie ai miei fantastici 4 nonni, Emilia, Arturo, Maria e Sergio, che sono sempre felici di verdermi e non vedo l'ora di poter visitare più spesso. Grazie ai miei amici della val di Fiemme che ci sono sempre stati per me. Anche se il tempo passato a casa non è stato molto negli ultimi anni è sempre bellissimo ritrovarsi e accorgersi che il tempo e la distanza non possono scalfire la nostra relazione.

Infine un grazie a Karin, per il suo perenne supporto e sopportazione, senza la quale sono sicuro non sarei riuscito ad arrivare fino a questo punto. Mi ha aiutato a rimettermi in strada dopo che mi sembrava di non riuscire più ad andare avanti. Come ti dico sempre, sei speciale!

Abstract

Electric scooters are gaining popularity as a means of transportation, especially due to their extensive usage by dockless rental companies. In the past, the Research Unit of Technical Dynamics and Vehicle System Dynamics of TU Wien has been studying the dynamics of e-scooters, particularly focusing on vehicle safety, and has identified significant potential for improvement, especially for braking manoeuvres.

Following these studies, it was deemed reasonable to aim for a brake assistance system specially configured for e-scooters, in order to improve their braking performance and braking stability. This was the starting point of this thesis, which will be specifically about the practical hardware realization of such a system to enable further research, while the related control strategies are the focus of an accompanying thesis.

Initially, the difficulties with braking identified by previous studies were concluded, followed by a careful identification of objectives and requirements for the actual assistance system. The goal is to create a system capable of assisting any rider, regardless of stature, strength, or driving experience, and dynamically adapting to external circumstances, such as road grip or the standing position of the rider on the footboard. The system should require only a single manual input from the rider, leaving them with the task of basically requesting a deceleration, while modulation and distribution of braking force to the front and rear wheel of the e-scooter is managed by the system itself to improve braking stability and safety.

Subsequently, systematic research was conducted to identify different possible solutions to the identified tasks, in order to effectively select a well-considered final concept. The working principles of potential solutions were also thoroughly analyzed from a technical point of view to solidly justify decisions during the development process.

The final system is a brake-by-wire system. It detects the operation of a single brake lever on the handlebar and after the control unit processes data from surrounding sensors, according to the chosen control strategy, activates electric actuators that engage two independent hydraulic disc brake systems. This thesis further deals with the practical realization of the chosen concept's prototype, including e-scooter, braking system of the front and rear wheel and secondary components such as wheel speed sensors. Equally important is the development and implementation of a system capable of determining the rider's mass and position on the footboard, which are crucial parameters for selecting the required total braking force as well as the optimal brake distribution.

Finally, the system ready for testing is presented as a whole, including an analysis of the achieved results and prospects for future steps in the project.

Contents

| | | |
|----------|---|-----------|
| 1 | Introduction | 1 |
| 1.1 | Motivation and objectives | 1 |
| 1.2 | Thesis structure | 2 |
| 2 | Literature review | 4 |
| 2.1 | E-scooter braking dynamics | 4 |
| 2.2 | Braking assistance systems | 5 |
| 2.3 | Brake-by-wire systems | 6 |
| 2.4 | Estimation of rider mass and centre of gravity position | 7 |
| 2.5 | Brake system dimensioning | 8 |
| 2.6 | Further literature | 9 |
| 3 | Braking and vehicle dynamics analysis | 10 |
| 3.1 | E-scooter model for braking dynamics | 10 |
| 3.1.1 | Equations of motion | 11 |
| 3.1.2 | Relevant braking scenarios | 14 |
| 3.2 | Brake system forces | 15 |
| 3.2.1 | Mechanical and hydraulic brakes | 15 |
| 3.2.2 | Rider braking force | 16 |
| 3.2.3 | Comparison and observations | 16 |
| 3.3 | Braking system dynamics | 17 |
| 3.3.1 | Ideal braking manoeuvre | 17 |
| 3.3.2 | Technical requirements for the braking system | 18 |
| 3.4 | Rider mass and position determination | 19 |
| 3.5 | Stepper motors | 20 |
| 3.6 | Analysis of existing brake assist systems | 21 |
| 3.6.1 | Anti-lock braking systems | 21 |
| 3.6.2 | Proportioning valve | 22 |
| 4 | Conceptual design | 24 |
| 4.1 | Prototype design approach | 24 |
| 4.2 | Clarification of task | 25 |
| 4.3 | Search for solutions | 26 |
| 4.3.1 | Brake force from rider | 27 |
| 4.3.2 | Brake force from actuators | 28 |
| 4.4 | Converge to the best designs | 29 |

Contents

| | | |
|----------|---|-----------|
| 4.5 | Reformulation of objectives and requirements | 30 |
| 4.6 | Design refinement | 30 |
| 4.6.1 | Hydraulic proportioning mechanism (v1) | 30 |
| 4.6.2 | Brake-by-wire system (v3) | 33 |
| 4.7 | Final design | 34 |
| 5 | Prototype design and realization | 35 |
| 5.1 | General concept | 35 |
| 5.1.1 | Choice of an e-scooter for a brake-by-wire system | 35 |
| 5.1.2 | Overall design | 38 |
| 5.2 | Rider input measuring device | 39 |
| 5.3 | Brake-by-wire system | 41 |
| 5.4 | Force-sensing footboard | 45 |
| 5.5 | Electronics and further sensors | 47 |
| 5.6 | Road friction determination and wheel speed measuring | 48 |
| 6 | Conclusions | 50 |
| 6.1 | Final prototype and project continuation | 50 |
| 6.2 | General considerations | 51 |
| 6.3 | Technical considerations | 51 |
| A | Appendix | 59 |

1 Introduction

Micro-mobility, involving short-distance urban travel, offers convenient and sustainable “first and last mile” options. Its attractiveness stems from flexibility, cost-effectiveness, and user-friendly characteristics [1], and, under the right circumstances, sustainability [2]. E-scooters, propelled by the global expansion of dockless e-mobility sharing services, have played a crucial role in the recent growth of micro-mobility. Worldwide e-scooter users went from 10 million in 2018 to 77 million in 2022, and projections indicate continued growth to 110 million users by 2025 [3]. This extensive growth has sparked numerous concerns, prominently focusing on problems like irresponsible rider behaviour, vandalism, riding space limitations, and, most notably, safety issues [4]. Considering that many riders through micro-mobility rental services are very inexperienced, it’s not surprising that the number of accidents has been steadily increasing [5] This fact underscores the need for a more in-depth study of these “new” means of transportation.

1.1 Motivation and objectives

The research unit of Technical Dynamics and Vehicle System Dynamics of the TU Wien has been addressing the dynamic behaviour of e-scooters in the past, studying their handling characteristics, creating models, and conducting practical tests to validate them. Studies especially on stability (in straight-line and steady-state cornering), steering behaviour, as well as braking behaviour, were carried out, providing significant and interesting results [6, 7]. While the stability properties were shown to be very similar to those of a bicycle, with self-stable behaviour at standard speeds, the emergency braking manoeuvre was shown to be critical, especially for inexperienced riders [8]. In other words, braking was identified as the first and most important aspect to address in order to improve e-scooter safety.

In the studies mentioned above, it was found that safety issues are not primarily attributed to the brake system itself, but rather to the rider’s skills. It was demonstrated that high deceleration rates are indeed possible when necessary, but require appropriate body motion moving the centre of gravity to the rear and a well-distributed braking force on both wheels, to avoid wheel skidding or overturning. However, given that most e-scooter riders are occasional users of e-mobility sharing services, a need for an assistance system that enables also inexperienced riders to come to a stop quickly and safely was recognized.

For these reasons, the research unit of TU Wien decided to develop a brake assistance system to address the entire braking difficulties with clear objectives in mind. These are the ability to adapt to any rider and help limit and distribute the braking force efficiently. The

goal is to have only a single brake lever, allowing the rider to set the desired deceleration, while leaving the task of adjusting an appropriate brake distribution to the assistance system, to enhance control and safety during the ride. This includes preventing wheel skidding and rear wheel lifting, as well as providing the rider with optimal vehicle control at all times.

A thorough literature research has been conducted to assess existing solutions or potential future approaches to improve e-scooter braking safety, but unfortunately, the research had limited success. Braking assistance systems like anti-lock braking systems (ABS) or combined braking systems (CBS) have been present on motorcycles for decades, but only in recent years have they begun to appear on bicycles, especially thanks to the growing popularity of e-bikes and s-pedeles. The presence of big accumulators in these vehicles, a feature shared with e-scooters, makes it inherently easier to introduce active braking assistance systems. It is not surprising, though, given the limited sources attesting to the study of electric scooter dynamics, that these measures have not been implemented on e-scooters yet.

For this reason, given that assistance brake systems already exist on other vehicles and many of their components are already available, it was decided to create a system specifically adapted to electric scooters. The system should be capable of adapting to a wide range of driving conditions and detecting the current riding situation through various mounted sensors, including current speed and acceleration, road friction coefficient, wheel speed, or rider centre of gravity position.

Developing such a system is a complex and comprehensive process, and this thesis, in particular, represents several steps towards these goals, which are the development of a working prototype of the brake assistance system realized on an actual e-scooter. In parallel and subsequent works of TU Wien, control aspects for this system will be addressed. In this thesis, the braking problem will be first analyzed in more detail, and then the process used to select the best solution will be explained. Following this, an explanation of how this concept was realized in real life and prepared for further studies on e-scooter braking safety will be provided.

Many solutions were analyzed to achieve these goals, and the final concept identified was a brake-by-wire system. This system measures the rider's braking input and converts it into an electric signal, which is then processed by the control unit along with data from sensors mounted on the vehicle. Depending on the detected driving conditions and the chosen braking strategy, the control unit electronically sets the braking torques on each wheel. This enables a highly flexible and independent use of both brakes, along with easily customizable brake actuation.

1.2 Thesis structure

Chapter 2 presents a literature review, where, due to the limited research on e-scooters, also works related to bicycles or, in some cases, motorcycles have been considered. The

fundamental sources used during this work are listed, ordered by themes, and their role in this project are explained.

Chapter 3 offers technical analyses and explanations of the physical principles behind the functioning of this braking system. In particular, e-scooter braking dynamics were summarized, which was necessary to gain background knowledge about this topic and make well-considered decisions during the development phase. The chapter includes detailed calculations of expected braking decelerations, forces and pressures and explanations of the working principles of the implemented components. Additionally, considerations based on the results obtained are provided to further upgrade understanding.

Chapter 4 deals with the key step of this work, namely the conceptualization of the final prototype. The systematic development process, starting from the initial requirements and ending with the final concept choice, is explained. Examples of alternative solutions evaluated and the reasons why they were eventually discarded are discussed here.

Chapter 5 addresses the realization and implementation of the braking system and the other systems necessary to make it work. First, it is explained how the theoretical concept developed in the previous chapter is concretely realized, and then the same is done for the surrounding systems, such as electronics or measurement systems. An overall picture of the vehicle and how all the developed and implemented systems work together is provided.

Chapter 6 presents concluding remarks of the project, including both personal reflections and technical reflections. Additionally, this chapter provides some predictions and recommendations for future works regarding this topic.

2 Literature review

This chapter provides an overview of the literature sources gathered and utilized throughout this master thesis and will be frequently referenced in the upcoming chapters. As of the current date, there hasn't been extensive research on electric scooters, given their relatively recent popularity growth. Based on the available findings, no braking assistance system has been developed for e-scooters yet. These are the reasons why this work frequently references literature on bicycles or motorcycles.

2.1 E-scooter braking dynamics

The little research on this kind of vehicle regards mostly the studies on the vehicle dynamics. Until now, only a couple of studies [9, 10] were conducted outside of those already mentioned from TU Wien [6–8]. Paudel [10] analyzes the scooter design and dynamics from a safety point of view, evaluating self-stability, handling and braking, also giving precious advice for future design improvements of the vehicle's geometry to improve self-stability. Garman [9], on the other side, investigates the rider-scooter interaction and its impact on vehicle control, coming to similar conclusions as the TU Wien studies regarding the influence of the rider position on braking performance. It was shown that, with the rider being significantly heavier than the vehicle itself, the riding style and the positioning on the footboard have a drastic impact on the stopping distance.

In this work, a simple model was used to analyze the e-scooter braking behaviour, as done by the previous TU Wien studies [6–8]. This simple model is the same as the one used by Cossalter [11], which, although initially designed for motorcycles, can be used for e-scooters as well and is suitable in describing the optimal brake force distribution between front and rear wheel, just taking the main factors, such as tyre-road friction coefficient, rider centre of gravity position, and current deceleration into account. Other papers containing simple bicycle models are [12] and [13].

There are also works that use more complete and complex models, as presented in [14]. This study takes into account the drag, lift, and pitch aerodynamic coefficients and longitudinal wheel slip, and implements the “magic” formula of [15]. In this research, optimal motorcycle braking for racing motorcycles is analyzed, which, like e-scooters, share the characteristic of overturning easily. Thanks to this work, all of these factors and their impacts were carefully assessed and evaluated to ensure that the assumptions made to simplify the system were well-founded. Specifically, tyre modeling will hold a crucial role in the upcoming projects

aimed at optimizing braking strategies, as elaborated in the parallel work of TU Wien by Matthias Riedl [16]. Also [17] displays a good example of how to find the braking limit of a racing motorcycle. A simpler yet interesting braking analysis of bicycles is carried out by [13], highlighting the main issues and dangers as wheel skidding and overturning, and proposing some potential improvements for vehicle safety, such as less powerful rear brakes or an anti-lock brake system.

2.2 Braking assistance systems

Braking assistance systems are common in motorized vehicles. However, despite decades of development and utilization in the motorcycle industry, their introduction to bicycles had to wait considerably, with the first appearance of commercial e-bike ABS such as those from Bosch [18] and Blubrake [19] only in recent years.

Such systems already exist on lightweight motorcycles, and some were checked to see if they could be adapted to e-scooters. The results show two interesting solutions, where two prototypes of electro-hydraulic pressure modulators are used. The first is a simple and compact construction, where the movement of the electric motor can decouple the brake lever from the brake caliper and actively modulate the fluid pressure by changing the volume of a connected chamber [20]. This way the driver does not feel the pressure modulation on the lever blade. The second modulator [21] operates on a very similar principle, but this time it incorporates additional valves to re-balance the pressure and safety check valves in the event of a power failure. This paper also shows an intelligent brake pressure control logic especially developed for this system. An alternative concept to the classical ABS principle is [22], which created a compact combined brake system for light scooters with cable brakes using a mechanical balance bar with a delay spring.

Also, several bicycle ABS projects can be found in scientific literature; the first one [23] is about research conducted in collaboration with Bosch, presenting the results of tests on bicycles equipped with an adapted motorcycle ABS. Braking tests are carried out first un-manned¹, then with a rider, and finally compared. The goal of preventing front wheel lockup and overturning is ultimately achieved, as extensively explained in the following PhD-thesis [24]. This work provides a comprehensive overview of the product's development phases and offers valuable information on the components and characteristics of hydraulic braking systems or the sensors used. The second one [25] explains the development of an ABS system and focuses mainly on its control strategies. More details about the construction and working principle of the systems can be found in the patents that followed this publication [26][27]. The system is very compact, with just a front wheel encoder², an electronic control unit, and an electronic braking actuator (a modified electrohydrostatic actuator). It is designed to be integrated only into the front brake line on any already existing hydraulic braking system, as the front wheel plays the most crucial role in hard braking. This research supported by

¹with a dummy instead of the rider and with an electric motor pulling the brake lever

²the above mentioned Bosch model needs also a second one on the rear wheel

Blubrake is interesting, especially knowing that in the years following its publication, the final product is proving to be valid and competitive in the market, especially for e-mountain bikes [28].

Other sources about bicycle braking assistance systems are experiments that try to prove the effectiveness of such systems with the purpose of research. One is from [12], and shows the integration of a motorcycle ABS on a bike. This paper is also helpful for the well-explained modeling of the bike and the control strategy, based upon three different pressure phases, increase–hold–decrease. An unconventional solution for cable brakes is presented in [29], modulating the braking forces by actively changing the length of brake cables with a pneumatic cylinder.

One last project is considered here, which describes a hydraulic brake proportioning system [30]. This solution, very different from the ones listed above, shows the possibility of splitting the braking lines of a single brake lever and proportioning the pressure between the front and the rear in order to improve braking performance. The key component is an automotive proportional valve, which, starting from a settable pressure, adjusts the pressure in the front and rear brakes according to a fixed proportionality factor. This setup demonstrates significant potential to enhance braking performance, allowing higher braking forces on the more critical front wheel and lower forces on the rear wheel, avoiding unnecessary rear lock-ups. However, no anti-lock or anti-overturning solutions are presented in this work.

2.3 Brake-by-wire systems

The final concept for the project is a brake-by-wire system, which is the reason why several existing examples are examined and considered. Very helpful is the review [31] to understand the current state of the art of brake-by-wire systems, as well as the most relevant ongoing research about the topic, listing the newest and most relevant research papers from ABS to brake-by-wire solutions. Also [32] provides a comprehensive and general overview of electronic braking systems.

An excellent example to understand the basic functioning of brake-by-wire systems for motorcycles is presented in [33], see Figure 2.1. Here, the main components and operating principles are shown. The system, specifically, uses an adaptive non-linear cascade architecture, meaning there are two loops (the inner for the position and the outer for the pressure) with a model identification for each loop. Using these models, the pressure controller tries to invert the nonlinear piston position–brake pressure relationship and an estimation algorithm guesses the temperature and brake pad wear, factors that influence heavily the non-linearities. Further details about this research can be found in a prior paper, [34]. Here the research focuses on the modeling of the electric and mechanical system, on the actuator friction identification and compensation, on the open-loop identification of the linear behaviour of the braking system as well as on the pressure control.

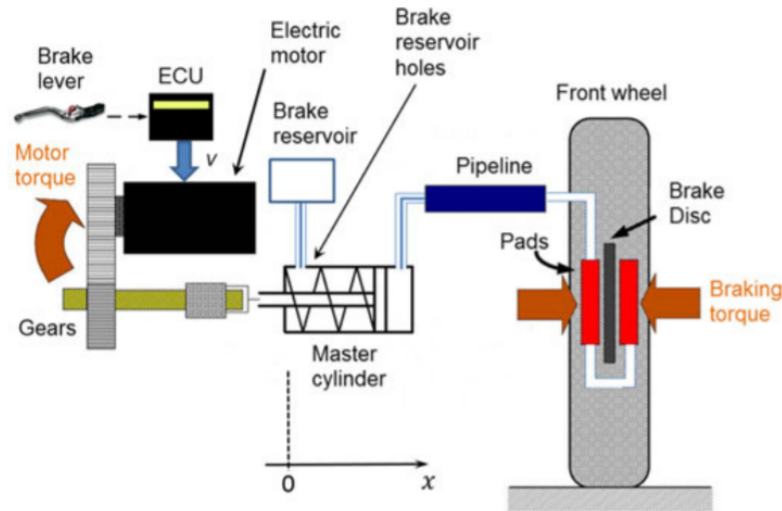


Figure 2.1: Schematic representation of the brake-by-wire system from Todeschini [33]

A similar system with a hybrid force- and position-control strategy was proposed and developed in [35], showing an interesting method of combining the advantages of these two control methods. The way this kind of control deals with the system's non-linearity is explained in [36]. Additional contributions to this topic are [37] and [38].

A further similar example is presented by [39], but this time for a passenger car. Here a motion control architecture with cascaded force, speed, and current control loops is implemented. The process of dealing with the non-linearities of the system with a cascaded control is well documented and suggestions for future improvements, such as a feed-forward compensation of the load-dependent friction force based on an accurate friction model are made. Another relevant research in the automotive field is [40]. In this paper, analogue to the sources mentioned above, the mechanical configuration is shown at first, and then the pressure control becomes the main topic of the research. The research goes very deep into detail, containing interesting inputs about the brake pressure–piston position curve estimation and various control algorithms to obtain a better dynamic performance.

A significant question in the development phase of the actual thesis is the pressure control in the brake lines. The work [41] is very helpful in the matter because it thoroughly compares position- and force-control in a hydraulic cylinder. Although the paper does not specifically address braking systems, many insights from it can still be applied to this thesis. An example for the estimation of the brake clamping force and a way to control it with an electric motor is available in [42].

2.4 Estimation of rider mass and centre of gravity position

As explained in [11], to find the optimal brake balance, knowing the vertical loads on the front and rear tyres is essential. However, since directly measuring these loads is complex

and requires additional sensors (see Section 3.4), this task can be replaced by an estimation of mass and total centre of mass position. This is an effective solution because it requires less hardware to be implemented on vehicles (compared to the solution presented in 5.4) and could therefore be also suitable for large-scale applications. The following sources will provide basic examples of how this estimation algorithm is supposed to work.

A good example of how a rider's mass can be estimated without directly measuring the weight can be seen in [43], where black and grey box approaches are demonstrated. For the grey box approach, the mass estimation occurs every time the rider demands full power with the throttle. To detect the full power request, an additional end-of-stroke sensor is needed. From the known maximum power of the motors and the measured acceleration and speed, one can directly compute the rider's mass by rearranging the longitudinal power balance equation. As for the black box approach presented, even fewer sensors are needed. The prediction relies on an analysis of the vertical acceleration. This has the advantage of being able to predict the mass in real-time but is not as accurate, as it can only reliably provide a range for the rider's mass.

Since the brake assistance system will also require, besides the mass, the (potentially) time-varying rider's position, an approach where the two quantities are simultaneously estimated has to be considered. This topic is explained in [44], where the mass (a constant quantity) of a heavy-duty vehicle is simultaneously estimated with the road grade (a dynamic quantity). The entire process is well illustrated, from justifying the model-based approach (instead of sensor-based) to the modeling and followed by the main part, the estimation. A recursive least square method with forgetting is used. Multiple forgetting, instead of single forgetting, is shown to work better, considering the different change rates of mass and road grade. However, no proof of convergence is provided.

A comparable study on simultaneous mass and grade estimation is presented in [45], where two algorithms are proposed. The first employs an observer, while the second utilizes a recursive least-square method with forgetting vectors, similar to the example above.

As will be explained in the following chapters (further details in Sections 3.4 and 5.4), no estimation will be employed at the project's outset. Instead, a force-sensing mechanism was developed to provide this data, while this type of algorithm will be developed and refined in a future work within this project.

2.5 Brake system dimensioning

A challenging aspect of the design phase in this thesis is correctly sizing the brake system, particularly given the limited space available on the electric scooter. For this reason, reference has been made to numerous publications on bicycle brake dimensioning, due to the absence of specific literature for e-scooters.

One of the most delicate tasks is creating a realistic model of the hydraulic disc braking system. In this instance, the research articles [13], [46], and [47] prove helpful, with the latter

also providing a detailed description of all main components of bicycle hydraulic disc brake systems. Additionally, the research by [48] is noteworthy, as it worked on a simulation model of a hydraulic braking system of a passenger car to identify crucial design parameters.

Estimating the physical force exerted by the human rider's inputs and the physical limits of common hydraulic bicycle brake systems has also proven to be a demanding task, and the related information can be found in [46], [24], and [49]. In particular, the paper [50] has been used for the final calculations as it provides precise measurements of all the components of the Magura MT4 braking system – the same system utilized in this project. It also offers good and concrete examples of the interdependence of brake pressure and volume absorption and a comparison between real-life and simulated data. The articles [51] and [52] also provide interesting insights into the most common mountain-bike hydraulic disc braking systems.

2.6 Further literature

A book that will be referenced multiple times and addresses various topics related to vehicle braking is [53]. Even though it focuses on braking systems for automobiles, it contains much knowledge and useful information that can be also applied to this subject. Additionally, research on the modeling and development of hydraulic components for braking systems is well covered in [54]. During the development phases, the study [55], which deals with bicycle braking analysis, has also been consulted. Various braking manoeuvres in different situations, alternating between front and rear wheel braking, are analyzed for performance. The conclusions drawn from this research can be highly beneficial in interpreting data and adapting results to the field of e-scooters.

Another key paper that helped improve the ergonomics, rider friendliness, and safety of the final vehicle is [56]. This is mainly a safety analysis of commonly used rental e-scooters with a few decisive conclusions that have been incorporated into this project's designs. A major example is the placement of the brake lever in the optimal position for the most natural, instinctive, and fast actuation possible.

Before entering the design phase, to ensure a more systematic, rational, and efficient approach, reference was made to the standard VDI 2221 [57, 58]. It covers all phases and offers numerous examples of product design processes that can be used as inspiration or directly adapted to almost any product—or prototype in this case—design project.

3 Braking and vehicle dynamics analysis

This chapter does not aim to explain braking and vehicle dynamics characteristics of e-scooters but rather focuses on analyzing the technical aspects that turned out to be crucial for the development phase of the brake assistance system. A more exhaustive and in-depth analysis of electric scooter dynamics will be found in the parallel work by Matthias Riedl [16]. His work is centred on developing a multi-body model of the vehicle, tyre modeling, and formulating (optimal) braking strategies for implementation on the e-scooter once this thesis is concluded.

3.1 E-scooter model for braking dynamics

First, one needs to understand the fundamentals of the vehicle's behaviour during braking manoeuvres. For this purpose, the model utilized in prior projects by Klinger [6], which is based on Cossalter [11], was utilized and slightly extended for this project's needs, including also a model to compute the forces acting within of the braking system.

Multiple assumptions and simplifications make this model suitable in this regard. The primary assumption is only considering straight-line driving manoeuvres. This allows the use of a much simpler planar model, neglecting all lateral forces and motions. Furthermore, the road gradient is also disregarded, as most e-scooters are predominantly used in urban areas

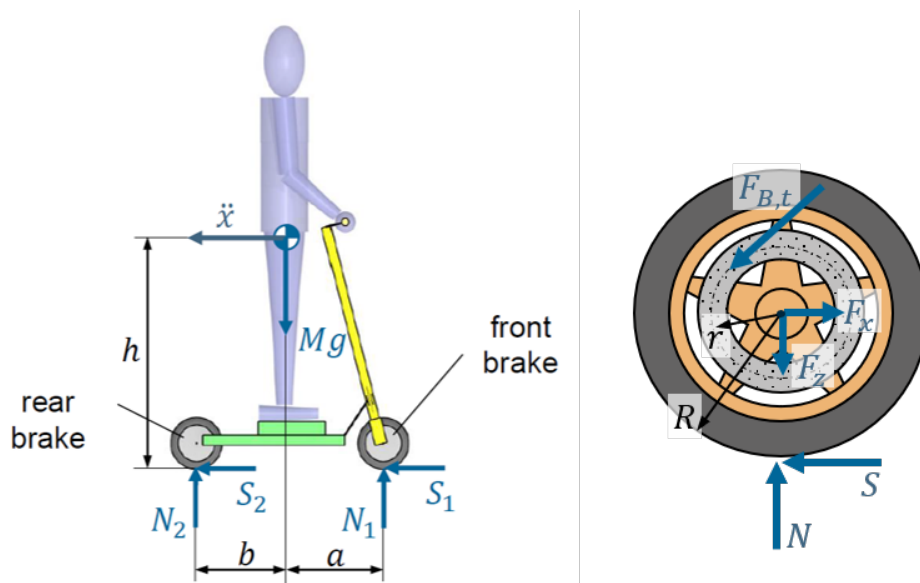


Figure 3.1: Model of the combination e-scooter-rider and the forces acting on the braked wheel. Forces normal to the shown plane as the clamping forces are not depicted

where roads tend to be relatively flat.

The tyre–road contact is intentionally simplified: the longitudinal and normal contact forces are assumed to be known, and the ratio between the two has to be below the maximal tyre–road friction coefficient. The same principle is applied to the interaction between brake pads and brake discs, utilizing experimental values for the friction coefficient while neglecting the size and shape of the contact patch and the influence of temperature changes. Finally, the influence of rolling and aerodynamic resistance is disregarded.

The combined vehicle–rider system is simplified and reduced to a single ideal rigid body, with the rotational effects of the (small) wheels neglected. To predict and model the rider, prior works utilized a Hanavan model [59], a mathematical representation of the human body. It was useful to find out the mass and centre of gravity position of the three exemplary riders’ physiques to be considered in the computations. The smallest and lightest rider was identified as the 5th percentile, the average rider as the 50th and the biggest and heaviest as the 95th percentile. This, combined with geometric data of the scooter Xiaomi MI M365 taken from [7], enabled the determination of the total mass and centre of gravity of the combined vehicle–rider system. All the data is available in Table 3.1.

| Rider and e-scooter parameters | Abbrev. | Value | Dim. |
|---|----------|--------------------------|------|
| Combined mass with 5 th perc. | M_5 | 76, 43 | kg |
| Combined cog height with 5 th perc. | h_5 | 923, 64 | mm |
| Combined mass with 50 th perc. | M_{50} | 89, 76 | kg |
| Combined cog height with 50 th perc. | h_{50} | 999, 52 | mm |
| Combined mass with 95 th perc. | M_{95} | 106, 41 | kg |
| Combined cog height with 95 th perc. | h_{95} | 1078, 55 | mm |
| Wheelbase | L | 830 | mm |
| Friction coefficient brake pad-brake disc [50] | μ_d | 0, 51 | - |
| Radius Wheel | R | 108 | mm |
| Radius Brake disc | r | 47 | mm |
| | | | |
| Variables | Abbrev. | Range | Dim. |
| Combined cog horizontal position | b | $173 \leq b \leq 613$ | mm |
| Brake balance | ρ | $0 \leq \rho \leq 1$ | - |
| Friction coefficient tyre–road | μ_r | $0, 4 \leq \mu_r \leq 1$ | - |

Table 3.1: The parameters used in the computations in the design phase

3.1.1 Equations of motion

As one can see in Table 3.1 and Figure 3.1, the essential parameters include geometric parameters such as wheelbase ($L = a + b$), the centre of gravity position (h and b), and total mass (M). During the design phase, the centre of gravity position was identified as the most critical parameter and was varied to identify critical scenarios, as thoroughly explained in Section 3.3. Additionally, brake balance ρ was introduced as a variable to enable the model’s utilization in examining the effects of various braking strategies on the system. Furthermore,

the friction coefficient between the road and the tyre was varied between the highest and lowest values used in [6], to analyze the behaviour under high and low grip conditions. To ensure the braking system's performance for all riders, computations were also conducted for individuals of smaller (5th percentile) and larger (95th percentile) statures, thanks to the Hanavan model. All parameters and variables used in the computations are summarized in Table 3.1¹.

The general approach is similar to Cossalter's, involving the computation of the normal forces on the tyres during a deceleration process. Assuming the rider is applying brake force to both wheels and the vehicle is not overturning, one can look at the equation of motion and also derive a formulation for each normal force:

$$\begin{aligned} M\ddot{x} &= S_1 + S_2 , \\ N_1 &= Mg \frac{b}{a+b} + M\ddot{x} \frac{h}{a+b} , \\ N_2 &= Mg \frac{a}{a+b} - M\ddot{x} \frac{h}{a+b} . \end{aligned} \quad (3.1)$$

From this formulation, the load shifts towards the front wheel during braking manoeuvres can be clearly explained. Additionally, the point at which the rear wheel starts to lift can be computed by determining the acceleration at which N_2 becomes zero:

$$\ddot{x}_{lift} = g \frac{a}{h} . \quad (3.2)$$

This represents the first physical limit that cannot be exceeded. Another significant one is the point at which the wheels start to lock up. This is primarily dependent on two factors: the normal force between the tyre and the ground and the current deceleration. The limit is defined as the tyre-road friction coefficient $\mu_{r,max}$, while the actual ratio is called braking force coefficient, as illustrated in the following equation:

$$\begin{aligned} \mu_1 &= \frac{S_1}{N_1} < \mu_{r,max} , \\ \mu_2 &= \frac{S_2}{N_2} < \mu_{r,max} . \end{aligned} \quad (3.3)$$

An important variable intentionally introduced to study the behaviour of e-scooters in various configurations and with different braking strategies is the brake balance. This is simply the ratio between the rear longitudinal tyre force and the sum of the total front and rear force, meaning $\rho = 0$ if only the front brake is active and $\rho = 1$ if only the rear is active.

$$\rho = \frac{S_2}{S_1 + S_2} = \frac{S_2}{M\ddot{x}} \quad (3.4)$$

From Equations 3.3, one can observe that the maximum longitudinal braking force is constrained by the road grip (assumed constant) and the normal force on each wheel, which

¹All data without notation is from the works of Klinger [6] and Vögl [7]

can vary with the mass and position of the driver and the deceleration rate (see Equations 3.1). Consequently, the maximum longitudinal brake force that can be exerted on each wheel is also affected by these parameters. Therefore, one must acknowledge that the full range of brake balance cannot always be physically achieved without the wheels skidding.

Cossalter also identifies the ideal braking maneuver, as one that evenly distributes longitudinal forces relative to the corresponding normal forces. This ensures that residual friction can be equally utilized to generate lateral forces on both wheels. Another advantage of this approach is that it enables both tires to reach their friction limit simultaneously, allowing the vehicle to achieve the maximum theoretical deceleration. In other words, the braking force coefficients μ_1 and μ_2 shown in Equation 3.3 should be equal. Assuming this, and that the friction limit is the same for both wheels, one can express the brake balance ρ considering this condition as follows:

$$\rho_{ideal} = \frac{a - h \frac{\ddot{x}}{g}}{a + b}. \quad (3.5)$$

From this equation one can see that the ideal brake balance can range from the weight distribution itself $\frac{a}{a+b}$ with no deceleration, towards zero with increasing deceleration. This means the required braking force on the front has to increase with increasing deceleration. This can also be seen in Figure 3.2, where the ideal brake force distribution is visualized in three cases, differing the standing position of the rider. To plot this non-linear curves the longitudinal brake forces of front and rear wheel are computed by rearranging Equation 3.4 with respect of the condition of the ideal brake force distribution 3.5.

$$\begin{aligned} S_{1,ideal} &= \frac{Mg \cdot b + h \cdot M\ddot{x}}{a + b} \cdot \frac{\ddot{x}}{g} \\ S_{2,ideal} &= \frac{Mg \cdot a - h \cdot M\ddot{x}}{a + b} \cdot \frac{\ddot{x}}{g} \end{aligned} \quad (3.6)$$

Furthermore, in Figure 3.2, the braking forces and decelerations were normalized. In this plot, the maximum tire-ground friction coefficient $\mu_{r,max}$ is assumed to be sufficiently high to prevent wheel skidding. If this was not the case, as deceleration increases, wheel skidding would occur before reaching the stoppie condition ($\rho_{ideal} = 0$), limiting the possibility of achieving higher decelerations. It's in these cases, that the rear brake plays an important role, as the rear normal force is still greater than zero, allowing the rear brake to contribute to stopping the vehicle.

Figure 3.2 and the corresponding Equation 3.6 demonstrate the complexity and sensitivity of a rider's task to maintain optimal braking force on each wheel, as these forces are different in every manoeuvre and continually change depending on current deceleration and standing position. More about the behavior of the brake system itself during such manoeuvres can be found in Section 3.3.1.

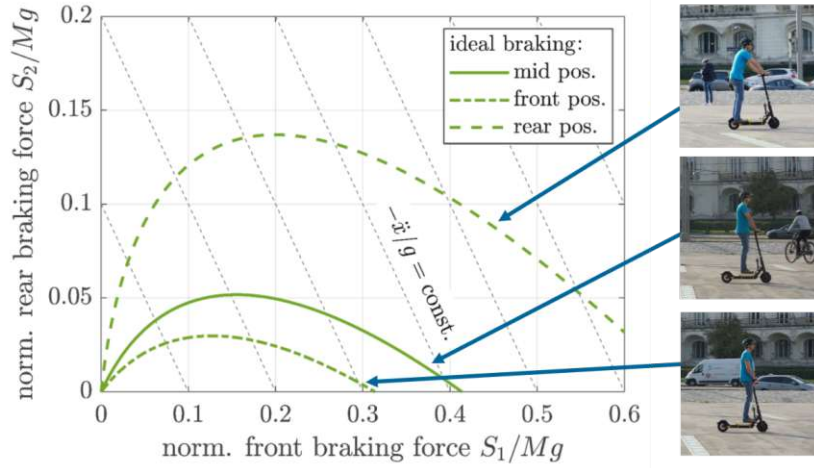


Figure 3.2: Ideal brake force distribution of different standing positions of the rider [60]

To fully describe the vehicle braking and dimension the brake system correctly, one must also look at the forces acting inside the brake system. This is the reason why the required brake force on the brake disc to achieve the desired deceleration with a specific driver mass, driver position, and brake balance were determined. The model used for this purpose can be seen in Figure 3.1 (right side), and the relationship between the longitudinal force on the tyre and the clamping force² on the brake disc of each wheel is:

$$F_{i,clamp} = \frac{1}{2} \cdot S_i \frac{R}{r} \cdot \frac{1}{\mu_d} \quad (3.7)$$

3.1.2 Relevant braking scenarios

With this model and these formulations, the braking of e-scooters can be comprehensively described taking the main factors into account. First, one can understand what level of deceleration is achievable, taking all the above-mentioned constraints into consideration. The maximal theoretical deceleration that can be reached with the heaviest and tallest driver (the 95th percentile) turns out to be 5.98 m/s², with the rider standing all the way to the back ($b = 173$ mm) and assuming high grip levels ($\mu_{r,max} = 1$). In this scenario, the limiting factor is the rear wheel lifting rather than the skidding of the wheels, which only occurs at much higher deceleration rates or at lower grip levels. However, under the exact same circumstances, if the driver moves to the centre of the footboard ($b = 392$ mm), the highest achievable deceleration before overturning is only 3.98 m/s², highlighting once again the significant influence of the standing position on these vehicles.

Looking at the literature, these computed decelerations seem higher than the most experimental results. For example, [61] found that the average deceleration of an e-scooter during an emergency braking manoeuvre is between 2.4 and 3.8 m/s². For reference, the bicycle regulation in Austria defines 4 m/s² on a dry surface starting from 20 km/h as the minimal

²The clamping force is acting from both sides on the disc normal to the shown plane in the same point where the tangential braking force acts on the brake disc.

deceleration for a vehicle to be allowed to drive on public roads [62]. But Klinger in [60] showed that, with appropriate body motion and good brake force application, higher decelerations (even slightly over 6 m/s^2) can be reached if the road conditions allow it. Based on these findings, it can be deduced that a deceleration of around 6 m/s^2 represents a significant but still realistic magnitude, which, if reliably reachable with the brake assistance system, would confirm the system's effectiveness. This deceleration was therefore taken as a target in the design phase to prove the system's benefits.

In this scenario, the driver is on the brink of overturning and can only brake with the front wheel ($\rho = 0$) as a result. The front brake of the vehicle must therefore be powerful enough to exert sufficient force to bring the whole vehicle and the rider, whose weight and size are above average, (being the 95th percentile) to a stop. Using the equations explained above, one can see that in this case, the clamping force must reach a magnitude of 1455 N.

There are many e-scooters that rely on electric motor brakes to stop. However, knowing the decelerations that these vehicles should reach, one can easily rule out the use of just this kind of brake on common e-scooters. This is because if a scooter has to start braking from its maximum allowed speed of 25 km/h with its maximum allowed power of 600 W [63], it would only be able to achieve a deceleration of $\ddot{x} = 0.96 \text{ m/s}^2$ for a 50th percentile driver, which is way too low to be considered safe. This explains why mechanical brakes were chosen for both wheels.

3.2 Brake system forces

3.2.1 Mechanical and hydraulic brakes

Mechanical or cable-actuated brakes have been the standard for bicycles for a very long time. The brake lever on the handle pulls a steel cable that brings the brake pads in contact with the braking surface, which is usually either the wheel rim or a brake disc. E-scooters have much smaller wheels than bikes, which is why cable-actuated brakes are typically either in the form of drum brakes or disc brakes. Among these options, disc brakes represent a system more suitable for this project because of their high power and responsiveness.

In disc brakes, the moving cable rotates a shaft that pushes the brake pads by turning its wedge-shaped end against sphere bearings in the housing. By taking the measurements of a common brake model³, the ratio between the cable tension and the brake pads' clamping force could be determined, which is around $i = 24$. This means that the clamping force acting on the brake disc is 24 times higher than the force needed by the rider to pull the lever blade. Additionally, since a common brake lever blade on the handlebar provides an extra mechanical advantage of around 3, the cable tension needed in such a brake system to achieve the target deceleration of 6 m/s^2 is around 8 times smaller than the required clamping force, resulting in 180 N of cable tensile force and 60 N of grip force.

³Model: Zoom DB680

Hydraulic brakes are commonly considered more effective and responsive than cable brakes and have the added advantage of being compatible with existing e-bike ABS systems. In this case, the mechanical advantage of the system doesn't only come from the brake lever itself, but also from the advantageous ratio of areas of the actuated piston and brake caliper piston. This ratio is 4.07, while the mechanical advantage of the lever blade is 5.78 (see [50]), resulting in a total mechanical advantage of 23.5. Consequently, the rider needs to apply a force of 61.5 N on the lever blade, while the force on the actuated caliper is 355 N, corresponding to 42 bar of pressure in the system.

3.2.2 Rider braking force

One of the project's goals is to make the vehicle suitable for a wide range of riders. The assistance system is required to assist everyone, including riders with smaller hands and lower grip forces, that are usually not able to operate the brakes with ease, but also very strong riders that can easily overbrake the vehicle. Some of the developed concepts, for the latter case, include the idea of having a system that works against excessive force applied by the rider. Quantifying the magnitude of the driver's forces is thus necessary to dimension the system correctly.

Literature sources found are about bicycle braking, which is appropriate since the braking system components of the two vehicles are often identical. In multiple emergency braking tests with different hydraulic braking systems performed by Kühnen et al. [51], it was observed that the average grip force of a grown rider during a hard braking manoeuvre, while still maintaining control of the vehicle, is around 120 – 130 N. This order of magnitude is further supported by Maier's research [50], where the maximal force that can be exerted in emergency situations is assumed to be 160 N. It's worth noting that this force might be slightly higher because it assumes an emergency situation with a strong rider pulling the lever blade spontaneously with full force. Additionally, in Maier's PhD-thesis [24], there is further evidence supporting this, demonstrating that hydraulic bicycle braking systems can achieve pressures up to 100 bar in emergency situations, corresponding to a grip force of around 150 N.

3.2.3 Comparison and observations

With grip forces on the order of magnitude of 150 N acting on the mechanical braking system of an e-scooter, it becomes evident that the cable tension exceeds the actually required level. Considering the mechanical advantage of the lever blade mentioned above, 150 N of grip force corresponds to 450 N on the cable, which significantly surpasses the necessary 180 N as calculated earlier. Similarly, for hydraulic braking systems, as mentioned previously, pressures up to 100 bar can be reached in emergency situations, indicating pressures that are more than twice the necessary value, as in Section 3.2 was calculated that 42 bar are theoretically sufficient for the significant target deceleration of 6 m/s^2 .

However, there is a key difference between bicycles and e-scooters that cannot be forgotten: the ratio between the wheel and brake disc diameters. Brake discs for e-scooters are not much smaller than their bicycle counterparts, while the wheel sizes differ significantly. This means that e-scooters, with a R/r ratio (see Figure 3.1) approximately double to that of a bike, require only half the clamping force on the brake disc to achieve the same longitudinal force on the tyres (see Equation 3.7). This explains the sizing of the brake systems for bicycles. On the other hand, e-scooters are twice as sensitive due to the wheel size difference alone. This implies that the same magnitude of brake lever force on an e-scooter would lead to inevitable wheel locking or overturning. This highlights another reason why braking with e-scooters can be very delicate and requires a significant amount of skill and experience to operate at the limit. Consequently, the development of an assistance system capable of limiting braking force makes even more sense in light of this observation.

This analysis reveals a significant difference between the strictly necessary braking force and the force a rider can exert on the system, with the latter being more than twice as large. Therefore, one can see that if a braking system is designed to compensate the entire force that a rider can apply⁴, then it must be considerably more powerful than a system that only needs to generate the strictly required braking force (such as a brake-by-wire system).

3.3 Braking system dynamics

3.3.1 Ideal braking manoeuvre

To design an efficient and effective braking system, one requires the understanding of the braking dynamics of the vehicle and rider as a whole, but also of the functionalities and dynamics of the braking system itself. To ensure that the final product can perform and deliver as intended, it is essential to comprehend the working principles of each component as well, in order to be able to design each one carefully.

The reference braking scenario analyzed for this task was once again derived from the work of Cossalter and integrated with some insights from Lie [13], as shown in Section 3.1.1.

The strategy is based on maintaining a constant braking force coefficient (see Equation 3.3) for the front and rear wheels. In other words, the ratio of the tyre's normal forces between the front and rear determines the magnitude of the longitudinal forces acting on each tyre, which are proportional to the clamping force required on each brake disc.

The effects of rider mass and standing position are shown in Figure 3.3. This figure illustrates the change in braking pressure with increasing deceleration, clearly demonstrating the effects of load shift. The axes in the plots depict the corresponding braking pressure within the hydraulic braking system, computed as explained in Section 3.2.1, assuming the use of Magura MT4 hydraulic disc brakes. The left plot compares two different drivers – the lightest (5th percentile) and the heaviest (95th percentile) – both standing at the centre of

⁴In a later stage of the design process it was decided that the widest possible range of brake balance has to be achievable at all times.

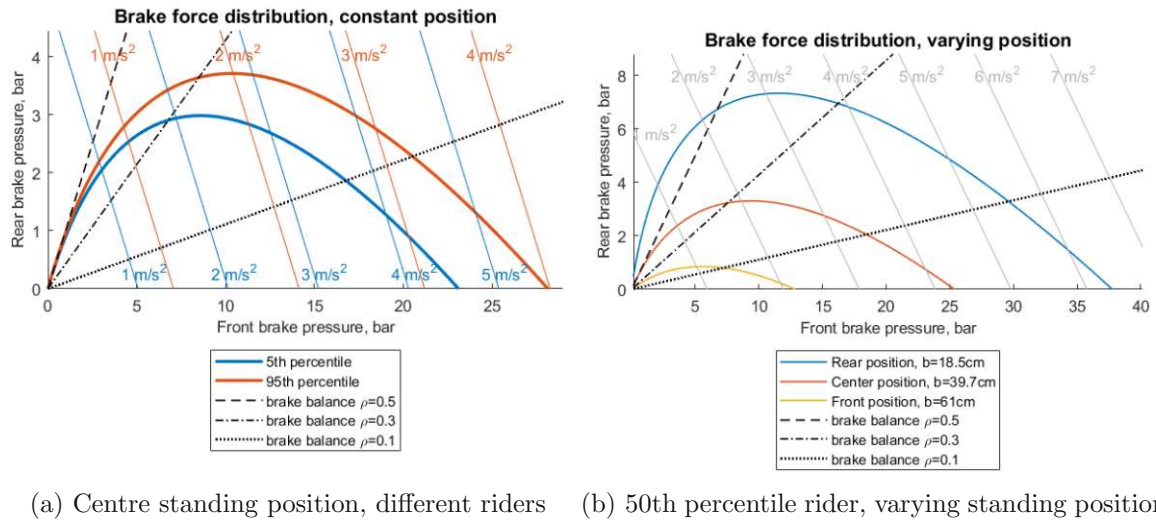


Figure 3.3: Brake force magnitude and distribution to keep the braking force coefficient of both wheels constant with increasing deceleration, $\mu_r = 1$

the footboard. On the other side, the right plot considers the average size of the Hanavan model (50th percentile) and compares three different standing positions: rider standing at the rear, in the centre, and at the front of the deck.

It's important to note that these plots were not used for system sizing (see Section 3.2 for that); they serve only to illustrate the basic mechanics of the braking manoeuvres and the braking system itself that will be encountered during the design process.

Looking at both cases, the noticeable load shift towards the front has the clear effect of making the driver rely much more on the front brake with increasing deceleration, up to the critical point identified as the highest-deceleration scenario in Section 3.1.2, where only the front brake can be used due to the rear wheel lift limit. It's important to note that the different stature of the riders doesn't affect the required brake pressure as much as the varying longitudinal standing position does.

3.3.2 Technical requirements for the braking system

This study underlines the importance of finding a way to compute the mass and center of gravity position to realize this braking strategy. Various options will be compared in Section 5.4, with the chosen solution being a force-sensing footboard capable of measuring the position of the rider standing on the deck.

Another crucial aspect to determine to ensure optimal braking performance is the friction coefficient between the road and the tyres. Since it cannot be directly measured, utilizing longitudinal wheel slip is a potential solution that could be explored in the future. For this reason, wheel speed sensors will be implemented, as described in Section 5.6. An alternative approach that will be considered is the use of a wetness sensor, capable of detecting water on the road surface, which might lead to a reduced friction coefficient.

Another interesting observation from Figure 3.3 is that with this braking strategy, the brake balance ρ rarely exceeds 0.5, occurring only with low decelerations and when the rider is positioned all the way to the rear. Consequently, proportioning valves or proportioning elements will always be placed on the rear brake line in the developed concepts of Chapter 4. Additionally, it's important to observe the common range of the brake balance for typical braking manoeuvres, which fall around 0 to 0.5. However, due to the research nature of the project, having as much flexibility as possible in setting the brake balance, even outside the usual ranges, will be a significant decision factor.

The final lesson that can be drawn from this analysis, for example looking at Figure 3.3, is that the range of pressure to be set for different situations varies significantly. The brake system will need to operate with adequate precision under diverse circumstances, so it will be crucial to select an actuator that can be equally effectively controlled under both high and low-load conditions.

3.4 Rider mass and position determination

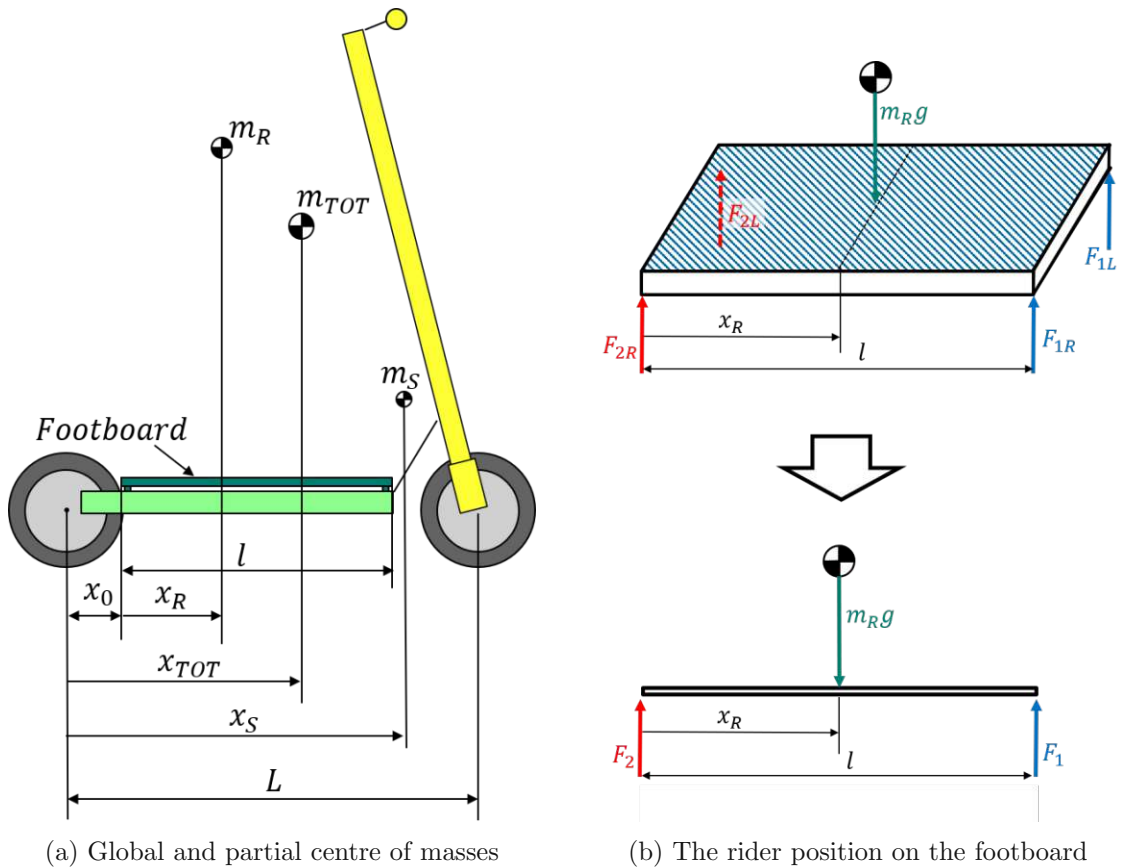
For reasons that will be explained in Section 5.4, a footboard with force sensors placed beneath will be used to determine the mass and position of the rider. This mechanism consists of a plate with four vertically guided legs in the corners, each of which has a sensor beneath that provides information about the force acting on it, as shown in Figure 3.4b. To determine the mass of the rider m_R , considering no vertical acceleration, the four forces simply need to be added together. The mass of the e-scooter m_S is assumed to be known, so the total mass of the rider-vehicle combination m_{TOT} is the sum of the two.

To find the longitudinal position of the total centre of gravity, the position of the rider on the footboard must be determined first. For this task, and to compensate for the fact that the spacial system is statically indeterminate, the two front and two rear forces are added, reducing the spacial problem to a planar problem. This can be done because the lateral position of the rider is of no interest here. The longitudinal position of the rider on the footboard can then be computed as a function of the measured vertical forces on the front and rear (neglecting the vertical acceleration from the road):

$$x_R = l \cdot \frac{F_2}{F_1 + F_2}, \quad \text{with } F_1 = F_{1R} + F_{1L} \quad \text{and} \quad F_2 = F_{2R} + F_{2L}. \quad (3.8)$$

This position indicates only the longitudinal position of the rider, with the reference starting position at the rear of the footboard (horizontal distance x_0 from the rear wheel hub), as shown in Figure 3.4a. To compute the longitudinal centre of mass position of the rider-e-scooter system, one can use the following equation, which incorporates the centre of mass of the e-scooter as well:

$$x_{TOT} = \frac{(x_0 + x_R) \cdot m_R + x_S \cdot m_S}{m_R + m_S} = \frac{(x_0 + x_R) \cdot m_R + x_S \cdot m_S}{m_{TOT}}. \quad (3.9)$$



(a) Global and partial centre of masses

(b) The rider position on the footboard

Knowing this, Equations 3.1 can be updated, with the normal forces on both wheels now dependent on the current rider mass and position. However, this method only applies to the longitudinal position, when the height of the centre of gravity of the rider needs to be accounted for as well. The actual solution is to estimate it from the Hanavan model, from which the correlation between the height and mass of people can be used.

Another aspect that will be taken into account in future is the fact that, as shown by [9], also the load exerted by the rider on the handlebar can be considerable in some cases.

3.5 Stepper motors

A significant aspect of the design phase involves selecting the appropriate type of actuator to operate the front and rear brake. The requirements for the motors in this project are rather unusual. The behaviour of a disc brake requires rapid overcoming of the air gap between pads and discs for immediate brake actuation in the first phase. During this movement, there is minimal resistance, which contrasts with the second stage of this process. Once the pads are in contact with the discs, only minimal movement occurs (due to the elasticity of the components and compression of the brake fluid in the case of hydraulic brakes. But the clamping force magnitude changes considerably in this case, needing to rise and adapt quickly and precisely. High pressure-setting precision is required during this phase, along with the ability to maintain a static torque at a specific level if needed. This nature of braking systems

must be considered for every concept involving an actuator during the design process.

Stepper motors were chosen for this application, mainly due to their precise control capabilities [64]. They can hold a specific torque with accuracy even in a static position, which is ideal for ensuring precise, reliable, and consistent braking force while the brake pad pushes against the disc. Their high resolution, thanks to microstepping, is also a significant benefit for such an application [65].

However, it's important to note that stepper motors are usually position-controlled, which can make it challenging to set a specific brake force during the second braking stage, as explained earlier. Setting a precise pressure by just adjusting position will require an accurate model for the nonlinear relationship between pressure changes and volume displacement, as explained in [41].

The solution to this problem was found in Nanotec stepper motor controllers [66], that have torque-control capabilities in addition to the common position-control. With this product, advantages of both these control modes can be utilized in the different phases of the braking manoeuvre. More about the motor model choice can be found in Section 5.3.

For reference, to understand the order of magnitude of these movements, one can consider the data from the Magura MT4 hydraulic brakes. The relationship between piston movement and pressure change can be modeled by considering fluid compression. Assuming a total brake fluid volume of $V = 40$ ml with a bulk modulus of $K = 1.4 \cdot 10^4$ bar, the piston (with an area of $A_{pist} = 85$ mm²) movement required to achieve a pressure change of $\Delta p = 1$ bar is as follows:

$$\Delta x_{piston} = \frac{\Delta p \cdot V}{K \cdot A_{pist}} \quad (3.10)$$

resulting in a piston movement of $34 \mu\text{m}$ to increase the pressure by 1 bar. This movement, in reality, may be slightly higher due to the elasticity of the system, but it remains very small. This characteristic allows the high-resolution stepper motors to operate comfortably and effectively without the need for a considerably large transmission system, unlike other motor types.

3.6 Analysis of existing brake assist systems

3.6.1 Anti-lock braking systems

Throughout the development process, many existing brake assist systems were analyzed based on related scientific publications, requiring a first understanding of their functionality to determine if they could be adapted to e-scooters or if they could be replicated and built from scratch. One of the most common and oldest brake assistance systems is the ABS (Anti-lock Braking System). This system is specifically designed for hydraulic braking systems and aims to maintain wheel slip within the optimal range to achieve maximum circumferential tyre forces possible.

This is done by adjusting the brake pressure set by the driver, which can be achieved in two primary ways. The first method involves temporarily redirecting part of the brake fluid to a brake fluid accumulator and then redistributing it to the system with the assistance of an electric pump or an electronically actuated piston. This solution is commonly used in passenger cars or motorcycles. However, e-bikes and e-scooters face challenges due to their smaller size and lack of a big power source like an engine. Therefore, a similar behaviour can be achieved by incorporating a single component called *pressure modulator* in line with the brakes. This modulator typically consists of a double-acting cylinder that counteracts pressure build-up by being moved against it by an electric motor, as explained in [67]. While there are variations in design that use different valve configurations, the working principle remains consistent. Although the performance of this second type of ABS may be slightly more limited compared to the first one, its relatively simple structure and compact size make it suitable for smaller and less powerful vehicles.

3.6.2 Proportioning valve

One method of assisting riders to efficiently distribute the braking force that was thoroughly analyzed during the design process is the use of proportional valves. These passive components are typically installed on the rear brake line and work to reduce the pressure on the rear brakes compared to the front, thereby preventing rear wheel skidding and improving braking stability overall. There are several variations of these valves, with the most relevant ones being fixed-setting pressure regulating valves and load-dependent proportioning valves [53]. It's important to note the difference to pressure-limiting valves. Proportioning valves can only change the ratio of pressure before and after the valve, while pressure-limiting valves limit the absolute pressure value and are commonly used in systems like CBS, see Section 2.2.

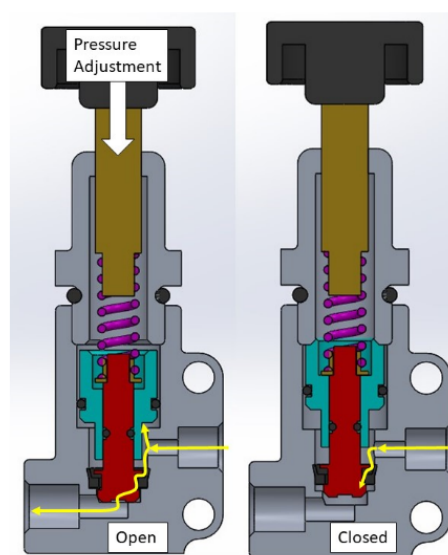


Figure 3.5: Working principle of proportioning valves [30]

3 Braking and vehicle dynamics analysis

Among the two types of proportioning valves, the load-dependent one was considered. As illustrated in Figure 3.5, the valve contains a piston that remains inactive under normal conditions. However, once a specific pressure threshold is reached, the piston partially locks and begins to set a specific pressure ratio defined by the areas on the two sides of the piston. This changeover pressure can be adjusted by varying the pre-compression of the spring connected to the piston, usually accomplished by turning a knob placed on top.

4 Conceptual design

4.1 Prototype design approach

As previously explained, solutions for e-scooter brake assistance systems have not yet been developed. However, brake assistance systems are not new; numerous similar systems have been designed for comparable vehicles, as outlined in Chapter 2. Each of these systems possesses distinct properties and is, of course, optimized only for its specific use case. Therefore, it is unlikely that among these systems, one will perfectly align with the needs of this project. Nevertheless, these solutions contain numerous interesting ideas and approaches that could prove beneficial. It's natural, however, that with every new project, there are unique and unprecedented challenges to overcome, requiring problem-solving capabilities and creative approaches. Hence, developing a final design that fully meets the project's requirements should involve a combination of innovative solutions and smart utilization of others' similar experiences.

Finding the optimal design when there are different ways to solve an issue is challenging, and a systematic approach is the way chosen to handle this situation. To make this process as efficient as possible, reference was made to the VDI 2221 [57, 58], from which examples and inspiration were drawn and used as a basis to develop a method specific to the needs of the project. There is no universal scheme because each project requires different steps and procedures, so the approach will vary slightly every time. This project, for example, does not aim to create a finished product ready for small-scale production; instead, it aims to efficiently and systematically compare different solutions without the need to develop any of them extensively. The goal is to develop a prototype that meets the initially set requirements but also leaves the possibilities for adaptations and tuning of specific parameters.

A schematic of the development process approach specifically created for this project can be seen in Figure 4.1.

The key aspect of the process discussed above is the big effort in **clarifying the task** by clearly formulating objectives and requirements. These objectives must be realistic and based on the current knowledge of the field, as well as comprehensive background research. The calculations outlined in Chapter 3 have primarily served this purpose, aiding in precisely identifying objectives and requirements. The more restrictive and precise the formulation, the narrower the research scope will be even before the start. Importantly, these objectives are not meant to stay static throughout the development process; they can also change and be adapted during the process, influenced by contextual factors or insights gained during the research.



Figure 4.1: The approach used to converge to the final concept

After establishing the objectives and requirements, the **search for solutions** including a comprehensive analysis of the situation can be initiated to explore and assess different problem-solving approaches. The identified variations are then elaborated, but care has to be taken to avoid excessive and unnecessary detailing of each variant. The aim was to refine them only to the point where they could be meaningfully compared.

The assessment and selection approach evolves with the progression of the process. During this initial stage, selection predominantly relies on an elimination principle. Given the multitude of possibilities, narrowing down the options is necessary to **converge to the best designs**. Naturally, the requirements set at the beginning also play a crucial role here.

Once the field is narrowed down, the **objectives and requirements are reformulated** more strictly based on the new insights gained up to this point. This shift marks a transition from the goal of convergence to **design refinement**. The designs left have to be reviewed more thoroughly to ensure they meet the now more strict demands.

After this refinement, which requires further considerable research and significant expansion of background knowledge, the **final design** can be chosen out of the remaining concepts.

This approach ensures careful consideration of various concepts and their thorough evaluation while avoiding wasting time on later unrealized concepts. It should minimize the risk of future implementation issues through a rational and systematic analysis of the situation, ranging from the system's overall view to its specific details.

4.2 Clarification of task

The initial objectives were based on the findings of the previous research on scooter dynamics conducted by TU Wien. As highlighted in the introduction, a significant potential

for improvement in braking safety and efficiency was identified. Based on these facts, primary objectives were formulated, indicating a direction to follow. These objectives can be summarized into four main categories:

- **From a vehicle dynamics perspective:** To assist the rider to optimize the braking manoeuvre within the limitation of the vehicle. Vehicle control and stability must thus be enhanced under normal and emergency driving conditions, particularly addressing issues such as skidding and rear wheel lifting.
- **From a vehicle control perspective:** To ensure consistent and reliable performance under all driving conditions, the system must adapt dynamically the actual road condition and rider mass and standing position.
- **From an ergonomic perspective:** To assist the rider most effectively, the braking action must happen intuitively and naturally and with appropriate operating forces. To further facilitate the brake actuation, the rider should be provided with a single input to set the braking request, leaving the complex task of optimizing the braking force modulation and distribution to the system.
- **From a research perspective:** To create a prototype to test different control strategies, test strategies of adaption to the circumstances and test acceptance of the system for various riders.

These objectives are naturally very general in this initial stage and will only serve to guide and narrow down the field of possible solutions. Additionally, to streamline the path toward the best solutions, further project-specific requirements need to be established, and each concept needs to meet them before undergoing a more detailed analysis.

4.3 Search for solutions

Once the goals are clarified and a distinct work direction is set, the search for the solution can be approached. The analysis of similar existing assistance systems discussed in Chapter 2 is helpful in identifying different categories and patterns to initiate the search in a systematic, structured, and comprehensive way.

This classification begins by identifying the different types of braking systems available on the market at the time of writing. According to [56], there are no standardized braking systems for e-scooters, with significant differences between models from technical and ergonomic perspectives. The most common ones are mechanical braking systems (also called cable braking systems), in the form of drum or disc brakes, followed by hydraulic systems. While the former are popular for their simplicity and affordability, the latter are typically found only in more expensive, powerful, and sporty e-scooters. This is because they offer superior performance and precision, but at a higher cost and complexity in terms of purchasing and maintenance.

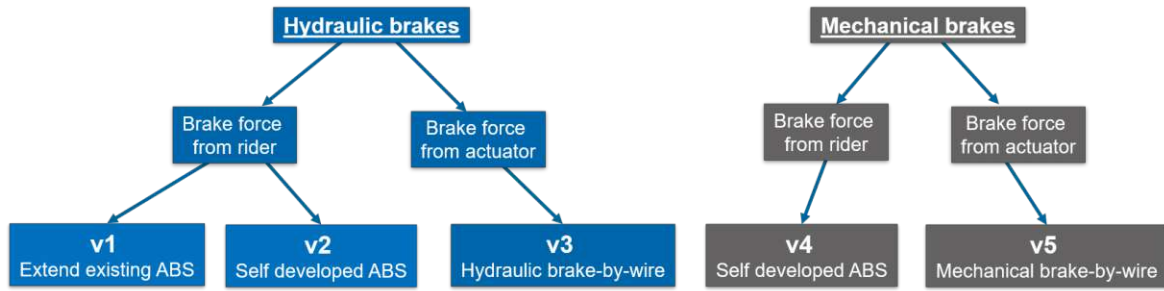


Figure 4.2: Overview and categorization of the main designs considered

As this brake type is gradually disappearing, another type is gaining popularity, which is the regenerative motor brake. Given that their use also results in increased driving range, this method proves to be widely adopted, though in varying quantities and modalities. While specific braking strategies diverge significantly, a consistent aspect is the limited recuperation power utilized, always leaving mechanical or hydraulic brakes to handle the more demanding manoeuvres. This is because, as concluded in Chapter 3, the very high power needed to suddenly stop a heavier vehicle at higher speeds cannot be entirely handled by the current road-legal vehicles. For this reason, motor brakes were ruled out for this project and not further considered.

A second category was then identified, namely with the way the braking force is applied. The hydraulic brake pressure or the cable tension is usually directly built up by the driver by pulling a brake lever on the handlebar, meaning an assistance system must be able to intervene and modify the input between the actuated lever and the brakes. An alternative to this common method is represented by brake-by-wire systems, where the braking force is exerted from mechanically uncoupled actuators.

To gain an overview of all possible solutions, a functional architecture was mapped, classifying the concepts with respect to the categories mentioned above. Some of these were just adaptations while others were new approaches. Figure 4.2 shows the five main types of solutions taken into consideration and structured by their functionalities.

4.3.1 Brake force from rider

The most common principle of safety system for rider-actuated brakes are hydraulic ABS systems. These systems, as explained in Chapter 3, are able to balance out the hydraulic pressure and have proven themselves also in the e-bike market, with Blubrake [28] and Bosch [68] being the most popular and advanced ones.

A simple and direct implementation of such systems on an e-scooter was considered (v1 in Figure 4.2), by taking advantage of the similarities between bicycle- and e-scooter hydraulic braking systems. However, simply implementing it would not meet the requirements, because the system, already equipped with its own sensors and logic, works independently and cannot be influenced in any way. Additionally, it was noted that ABS systems are active only

during emergency situations, while the project goal was to improve braking under every circumstance, not only emergency braking. This implies that for the ABS to be integrated and still have a system that meets the requirements, it would need to be extended with further functionality. This means implementing a brake balance setting system capable of fine-tuning the brake balance at all times, while the ABS would take care of avoiding excessive slip and overturning.

An alternative to controlling the brake balance while also incorporating an anti-lockup and anti-rear wheel lift device is to develop a hydraulic ABS system from scratch (v2 in Figure 4.2). The design of the brake pressure modulator proposed by [20] appeared to be the only feasible option, given its compact and simple construction. The system should be mounted on both the front and rear braking lines, and by independently limiting the pressure on the two wheels, the brake force modulation could be adjusted.

CBS systems, popular safety features for motorcycles' hydraulic brakes, were also considered but were quickly ruled out because they don't allow dynamic adjustments. However, this system has significant potential, as confirmed by the upcoming launch (in 2024) of the first commercial bicycle version by Magura [69].

The same principle of limiting the braking force set by the rider to avoid blocking and overturning can also be applied to mechanical braking systems (v4 in Figure 4.2), meaning it must be possible to reduce the tension of the cable if needed. While replicating the pneumatic system proposed by [29] seemed unrealistic for a small vehicle like an e-scooter, compensating the cable force by using an electric motor working against it appeared to be a more feasible solution. The previously addressed issue of the very high forces a grown rider can exert on a brake in emergency situations (see Section 3.2) can be addressed by choosing the right combination of levers to gain enough mechanical advantage to counteract them. To have a complete solution, this setup should be extended with a further mechanism to make the brake balance adjustable. This matter could be addressed by implementing a brake bias bar, a very common feature of go-karts and race cars [70], to the already existing lever mechanism, to move the cables' attachment points relative to each other.

A challenge of the systems with the brake force coming from the rider is the task of working consistently while having to adjust to unpredictable and unique styles of braking. A simple solution of this problem can be offered by systems where the brake force is exerted by actuators.

4.3.2 Brake force from actuators

Brake-by-wire systems (v3 and v5 in Figure 4.2) bypass the issue of dealing with the rider's grip force completely by building up the braking force independently from the actual force the driver exerts on the lever blade, giving the system a higher level of freedom and repeatability. Such systems work by converting and processing the driver's braking request into an electric signal, which drives actuators that engage the brakes independently from each other,

making it very easy to manage brake distribution. Anti-lockup and anti-overtake features are naturally incorporated, since not only the relative distribution between front and rear can be set, but also the force's absolute value, making a force-limiting feature redundant.

Not having to account for the forces exerted by the rider on the brake lever presents both advantages and disadvantages. On the positive side, it allows for a high degree of freedom regarding the ergonomics of the brake lever actuation. Especially to accommodate riders with small hands or low grip strength, it's simple with these systems to adapt the shape and hardness of the lever, since they are not critical for determining braking force.

However, this freedom brings along a problem: even though one can try to emulate it, it will be impossible to recreate the haptic feedback from the braking system to which we are all accustomed.

4.4 Converge to the best designs

Once it was ensured that all the considered designs respected the general requirements, a first screening could be conducted. Designing and implementing an ABS from scratch (as for v2), for example, would make the project diverge from the research objectives that were clearly set at the beginning. The focus should remain on developing a system for research purposes and investing a lot of effort in building such a product from scratch without prior experience and guarantees of effective functioning makes this potential solution unsuitable for this specific case.

To further narrow down the number of feasible solutions, a comparison between hydraulic and mechanical brake systems was carried out. In particular, the features relevant to the previously formulated objectives were analyzed. One of these is ergonomics, specifically the requirement that the system's usage must be suitable for all users. A characteristic of cable braking systems, for example, is the constant presence of friction among all mechanical components, especially the steel cable with the bowden tube, which can make operating the brake lever more challenging and inconsistent.

From a system control perspective, another unique issue with mechanical systems is the complexity of measuring braking force. In this case, it would mean measuring the tension of the cable, a very small component subject to large forces and continuous movement. In comparison, measuring the same quantity in a hydraulic system is simple, it is sufficient to install a pressure sensor and convert it to braking force by knowing the cross-sectional area of the piston. For these reasons, the mechanical ABS (v4) was not further considered.

A similar analysis was carried out for the brake-by-wire system. In this instance, both hydraulic (v3) and mechanical (v5) systems were evaluated and compared. Although both systems share similarities, utilizing the same type of actuator and demonstrating comparable behaviour, the reduced friction of hydraulic systems is considered advantageous to mechanical systems. Another minor advantage of the hydraulic system is that, even though it would be redundant, it would still provide the possibility to conduct tests with an integrated ABS.

Therefore, considering these factors and the simple method of measuring braking force, it was decided to proceed exclusively with hydraulic braking systems, either by extending an existing ABS (v1) or by implementing a hydraulic brake-by-wire system (v3).

4.5 Reformulation of objectives and requirements

From this initial analysis, certain points that need to be considered for the continuation of development have been identified. First and probably most important is the realization that a driver force-reducing system, such as an ABS, was not the only way of solving the issues faced. Of course, implementing an already working e-bike ABS and adapting it to an e-scooter would have many advantages, but so would a brake-by-wire system.

To converge to a final design, stricter requirements are needed, based on the findings from the non-stop parallel background research and the analysis of many possible solutions. Only finding designs with functionalities that meet the general requirements is not enough anymore; a concrete and more detailed version of them has to be developed to ensure that the final decision is based on solid and objective facts.

The potential of some of the evaluated concepts, for example, shows that it is possible to gain complete control over the brake distribution (see Equations 3.6), enabling a full range of ρ between 0 and 1. This ability is considered useful for future studies on braking strategies and was therefore set as a new requirement from this point on.

It was also decided that the most effective way to achieve maximum braking control is to have two disc brakes on the scooter, introducing the next new requirement. These brakes are powerful, already available on many models, and would allow identical force application on both wheels, which would make the whole system simple to design and manufacture.

Before choosing the final concept, one also has to ensure there is a concrete way of realizing and implementing the chosen design, checking for the size and availability of the crucial components. Also, the ergonomic point of view cannot be neglected, as both remaining concepts should allow universal use for people with different size (especially regarding the hands) and grip strength and offer a clear improvement compared to traditional braking systems.

With also these further two additional requirements defined, concerning feasibility and ergonomics, the target for the refining process of the last two remaining concepts (v1 and v3) was set.

4.6 Design refinement

4.6.1 Hydraulic proportioning mechanism (v1)

The first design to be analyzed more deeply was the implementation of an e-bike ABS with the added function of setting the brake balance. Proportioning valves are a simple and popular solution to adjust the brake distribution in hydraulic systems. These valves are typically found

in cars with dual-circuit braking systems, specifically on the rear brake line with the purpose of reducing the braking pressure to prevent the rear wheels from skidding (see Section 3.6). Research by Michael D. Machado [30] demonstrated that this system can also be effectively implemented on a bicycle, showing some potential for improvement in braking performance. It also confirmed the initial idea of combining an adaptable proportioning functionality with an ABS, stating that “*the ideal system for minimum stopping distances would include a weight-sensing proportioning valve, an anti-tip-over valve, and a front wheel anti-lock-braking system*”. Automotive proportioning valves are readily available on the market, and their pressure rating is sufficient to withstand 100 bar or more, which can be reached during an emergency braking manoeuvre (as analyzed in Section 3.2). An electric motor could be used to turn the knob of the valve and adjust the changeover point.

However, a significant limitation was identified in these systems. The proportionality factor that these systems can achieve is a fixed factor, determined only by the ratio of the two frontal areas of the piston inside the valve. This ratio, corresponding to the reduction factor once the changeover pressure is reached, cannot be changed and typically ranges around 43% for the most common models [71]. This means that, depending on the pre-loading of the spring in the valve and the current pressure, the range of brake distribution is only $0.3 < \rho < 0.5$ (see Figure 3.3b for reference). Since the proportioning is constant, achieving a larger range would necessitate the addition of more valves to the system. For instance, adding a valve on the front line could increase the range to $0.3 < \rho < 0.7$ and allow for higher pressures on the rear brake if needed. However, one can not easily achieve a much bigger range with this specific type of valve by connecting them in series; it would not be particularly effective because the proportioning effect of each added valve diminishes relative to the previous one. Furthermore, using more valves would significantly increase the complexity of the system, as each valve would need to be separately driven and controlled by a motor. Thus, the system’s limitation of allowing only small adjustments can only be partially improved by using more valves. As the new conditions required the full brake distribution range, this version was discarded.

The working principle of such proportioning valves, as thoroughly explained in Section 3.6, affects the pressure in a braking line by essentially utilizing a small inline double-acting hydraulic cylinder with a specific ratio of its two frontal areas. However, it was observed that the pressure differential before and after this cylinder could also be influenced by an external force acting on this cylinder. This new alternative approach was then further explored due to the promising advantages it showed. The specific idea was to place a common double-acting hydraulic cylinder on the rear braking line and adjust the front-rear distribution of brake pressure by exerting a variable force on the piston (see Figure 4.3).

The control of the distribution would be constantly adapted by the piston, allowing it to always set the desired distribution as required throughout its whole spectrum. The only limiting factor to allow the use of the complete range is the driving motor power. This must indeed be enough to counteract the pressure exerted by the rider to allow, for example, the

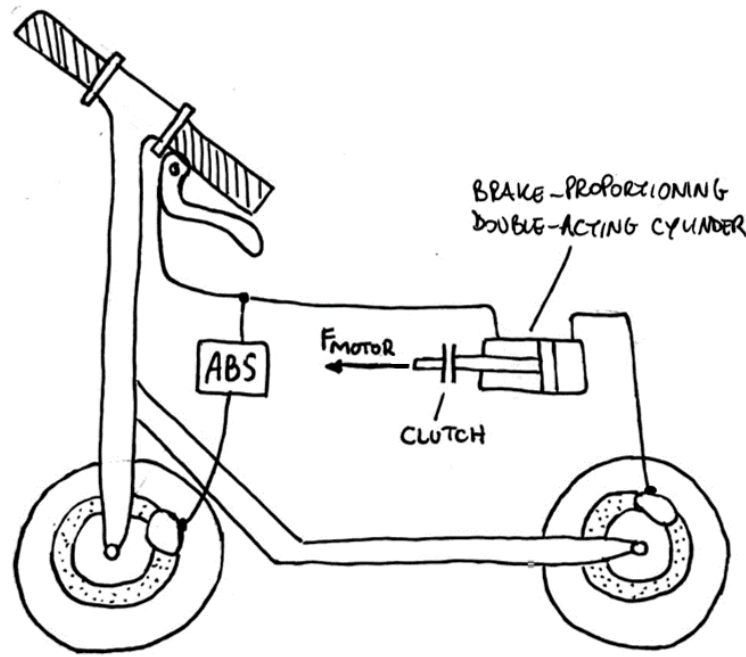


Figure 4.3: Schematic of the hydraulic proportioning solutions

use of only the front brake. The single input of braking pressure would always come from the rider, who by acting directly on the brake lever would also receive haptic feedback to feel the influencing action of the system.

In addition to this, the system behaviour would be beneficial even when not active. With the piston free to move even with the engine not electrified, a preset reduction by the ratio of the two frontal areas of the piston¹ would reduce the pressure on the rear by default, acting as a fixed proportioning valve. If energized, the system would, therefore, optimize the braking dynamics in normal driving situations, with only relatively small forces exerted on the system necessary, since the action would be double, with a simultaneous increase in pressure on one side and reduction on the other.

To increase braking effectiveness in emergency situations, the piston could shift the pressure to the more effective front brake if the force exerted by the pilot on the lever was not deemed sufficient. If the pressure exerted by the pilot instead was too high, the single ABS system, placed on the front, would reduce it. The system, in fact, would make the implementation of a second ABS on the rear unnecessary, having the possibility, if desired, to avoid skidding even there, shifting the excessive pressure to the front where the ABS system would reduce it as usual.

Furthermore, the system proves to be interesting because it would be very effective even without the use of an ABS system. While the braking distribution setting would work in a similar way to the system just explained above, when the pilot's pressure becomes excessive, the appropriate action of the piston would decrease the longitudinal force on the front wheel

¹The piston to be used would be a simple commercial double-acting cylindrical piston; therefore, the area of the piston head on the rod side would necessarily be smaller than the section of the cylinder.

until just below the skidding limit, shifting the remaining pressure to the rear. This would then bring the rear wheel to lock up always before the much more critical front, which could be, for example, avoided by introducing a pressure limiting valve on the rear line. This way, vehicle safety would still be considerably increased, being able to actively adapt the brake distribution and avoid wheel lock-ups without needing a complex hydraulic system like an ABS. The type of motor to be used in this case has been identified as a stepper motor, for the reasons explained in Section 3.5.

To ensure the feasibility of this concept, the existence and availability of a simple double-acting cylinder capable of withstanding pressures up to 100 bar was confirmed. One factor to pay attention to is the method by which the cylinder is actuated. As mentioned earlier, for the braking system to operate even without the motor being turned on, the piston must be able to move freely. This necessitates implementing a way to disengage the motor on command, as a clutch or a brake that is active only when energized, to release the piston from the inertia of the motor.

4.6.2 Brake-by-wire system (v3)

On the other hand, there were fewer details to investigate for the second concept in question, the brake-by-wire system. After all, the system is conceptually quite simple, and there is no need for a deep investigation from the working principle point of view. However, the details to be reviewed concern the new, more restrictive requirements that have been defined.

One of these concerns is ergonomics and the aim of making the braking command as simple and intuitive as possible for the pilot. Unlike the previous system, which relied on the classic use of the brake lever physically connected to the assistance system to provide haptic feedback on the degree of actuation, the brake-by-wire system does not have this advantage. To achieve the necessary requirements, simply adding a button, like the throttle potentiometer, would not be enough. Instead, the classic brake lever, like that of a bicycle, would still be used. A mechanism has to be developed to measure the rider's input, capable of adapting the feedback of the actuation to emulate the feeling of brake pad compression. In addition to this, it should also be possible to implement a stopping feature that gives an intuitive sensation of reaching the end of the stroke, indicating to the rider that the system is about to try to stop the vehicle as quickly as possible. Combining all these functionalities has proved to be achievable, reusing a common lever blade of a mechanical bike brake to maintain the actuation mode to which everyone is accustomed, and measuring the cable movement to determine the desired deceleration. To give a realistic and natural braking feeling to the driver, the cable is attached to a linear guided element and supported by a spring with specific stiffness, carefully chosen for this purpose, as shown in Figure 4.4. This element needs to have a travel stopping spot at a precise point to indicate to the rider the achievement of maximum braking power. If well-built, this system would also allow the rider to adjust the lever hardness as desired depending on his/her preferences and physical strength by changing the pre-loading of the spring.

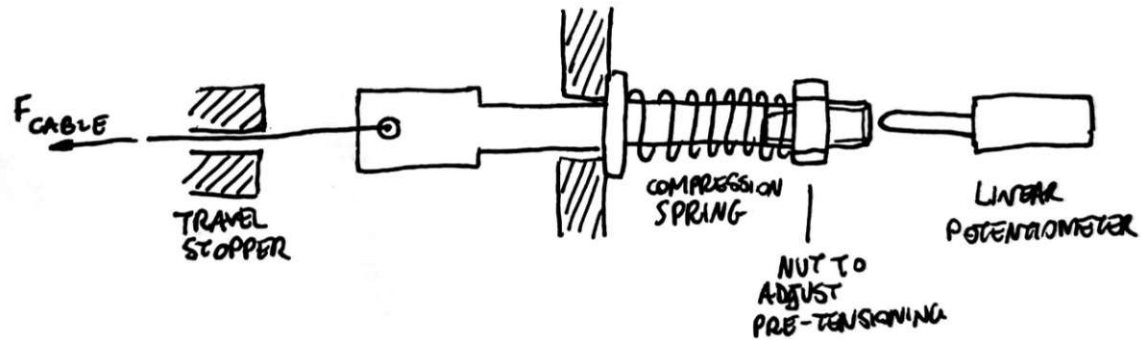


Figure 4.4: The working principle of the rider input measuring device, to detect the desired deceleration and still give a natural and adjustable feel to the rider

As previously discussed (see Section 3.5), reliance would be placed on stepper motors as driving units. They can actuate the piston of a cylinder of an existing hydraulic bicycle brake system, allowing the system to be realized using mostly existing and reliable components. This version would also simplify the piston thrust mechanism, making the construction of a complicated mechanism with brakes/clutches and gear and racks unnecessary, as in the previous case.

Of course, it is clear that the system is not able to work in the absence of electricity, making it extremely vulnerable and unlikely for future large-scale implementation. A simple solution for the lack of a backup brake can be the addition of a classic footbrake, very popular on classic non-motorized scooters. However, this factor does not have a huge relevance in this project, which, as already mentioned several times, has mostly research purposes.

4.7 Final design

Both concepts underwent extensive development and refinement to ensure they met all requirements. They diverge significantly in many aspects, resulting in distinct advantages and weak points. On one hand, a system capable of assisting the rider, enhancing existing ABS functionalities and improving performance even when unpowered. On the other hand, a highly adaptable and effective system, that offers high flexibility in braking strategies. Its standout feature is its ability to almost entirely relieve riders of traditional braking tasks, leaving him/her only the job of requesting a specific deceleration while managing all other aspects autonomously.

Ultimately, the brake-by-wire concept was selected for its unparalleled freedom. It offers direct control not only over brake distribution but also the brake force modulation, providing a level of versatility unmatched by the alternative concept.

The control for this braking system is to be managed by a central control unit onboard (a Speedgoat Unit). All sensors and control strategies are intended to be processed by the Speedgoat, where MATLAB and Simulink models can be directly implemented, serving as the computing controller for the entire e-scooter.

5 Prototype design and realization

This chapter demonstrates the realization of the carefully chosen braking assistance system concept. Practical solutions are shown to maintain the idealized working principles defined in the previous chapter within its physical limitations. The process of designing or selecting the most suitable components for this task is the main focus of this chapter. Subsequently, the assembly and implementation of the different elements will be reviewed and evaluated as well.

5.1 General concept

For the selected brake assist system concept to operate effectively, the surrounding environment must be adequately designed to enable its full potential utilization. This includes choosing a suitable vehicle, providing the necessary signals for the controls, strategically positioning all necessary components for an undisturbed ride, and enabling easy tuning and maintenance of the system for future research purposes.

5.1.1 Choice of an e-scooter for a brake-by-wire system

The Research Unit of Technical Dynamics and Vehicle System Dynamics, as mentioned, already possesses an e-scooter (Xiaomi MI M365) equipped with sensors and measurement technology, which was utilized for previous research on e-scooter dynamics. The geometry of this e-scooter was also referenced in Chapter 3 for the dimensioning of the brake system. However, for this project, a new vehicle was selected to find a more suitable one while keeping the old one intact and ready for use. Throughout the prototype design process, the most important characteristics of the ideal vehicle have already emerged, as well as the less critical qualities. Key requirements for the new brake-by-wire-e-scooter are the following:

1. **Dual disc brakes:** The most efficient way of bringing the vehicle to a stop was identified as disc brakes. For simplicity and consistency reasons, it was decided that the front and rear brakes should be two identical systems.
2. **Ordinary model:** For the research to be relevant to most of the currently available e-scooters, an exemplary model with typical geometry and wheels was needed.
3. **Space for measuring and actuation equipment:** The vehicle must physically allow the implementation of various components such as electric components, brake assist system, and various sensors.

4. **Power:** For research purposes, a vehicle that can comfortably reach and exceed the common speed limit of 25 km/h should be used. This is to test the limits of the system itself and to ensure proper functioning at these speeds by designing it for a slightly wider operating window. Ideally, the vehicle has a road-legal and “open”-mode with no speed limiting that can be selected.

With these main requirements, the choice is already narrowed down significantly, but there are still many other distinct characteristics that differentiate the models from each other. The following (secondary) aspects were also evaluated and used to restrict the final choice to one single model:

- **Wheels and tyres:** The maximum wheel size allowed was decided to be 10”. Larger wheels would feel unrealistic and deviate too much from the model used in the computations. Air-inflated tyres were preferred over solid ones, while there was not much relevance identified between tube and tubeless models.
- **Motors:** Ideally, a front wheel motor would be advantageous for this project to leave the possibility open for effective use of regenerative braking as a supplementary help. However, since the desired motor power was slightly above average, most models in this category had either rear-wheel or dual-wheel drive, with the latter being considerably more expensive.
- **Brakes:** Hydraulic disc brakes on the e-scooter are preferable, but mechanical disc brakes are acceptable as well if they can be removed and switched to a hydraulic system.
- **Suspensions:** While suspensions provide a very comfortable ride, they were not desired for this project because they add additional degrees of freedom that make the system less predictable. This would require, for example, a multibody model that is more complex than the one planned for use in the braking strategy control. In case the model has springs or dampers, these could be replaced with stiff rods.

The final choice was made selecting the *Rapido Serie Oro* model from the company MV Augusta [72], shown in Figure 5.1. This scooter appeared to be the best compromise when comparing all factors, meeting all fundamental requirements, and offering several nice-to-haves to facilitate the development of an efficient braking system.

The e-scooter has two 10” wheels with tubeless tyres, and two mechanical disc brakes with 120 mm rotors¹ that have the standard size of mountain bike brakes. This will allow a free choice of a specific and project-fitting hydraulic brake system model to be quickly and easily swapped for the original one.

The frame of the vehicle includes a very spacious deck, which is very comfortable but has the small issue of being slightly inclined, probably for ergonomic or aesthetic reasons. The fact that it is not perfectly flat will be addressed later on in Section 5.4. The vehicle has many

¹They are actually semi-hydraulic brakes, a mechanical-hydraulic hybrid, with a normal cable running to the brakes, where it actuates a hydraulic brake cylinder (model: ZOOM HB 100 XTech)



Figure 5.1: The chosen Vehicle for the project, a MV Agusta Rapido Serie Oro

details mounted on the main frame (some sort of wings on the front, fenders, and a number plate holder on the rear), which offer very useful mounting points if they are disassembled. The frame is specifically developed for this model and is made out of a magnesium alloy to make the scooter relatively light for its size and, in our case, allow processing if some modifications have to be made.

The brushless DC motor is placed on the rear and has a nominal power of 500 W but with peaks up to 1000 W. This vehicle is supposed to be road-legal and therefore it cuts the power as soon as the 25 km/h mark is reached. However, the producing company offers an additional "Power Key" that unlocks the usage of the full power (hence making it not road-legal anymore). This is supposed to be used only in private, protected environments, and allows reaching speeds of up to 38 km/h. This is a very good trade for the project because the scooter itself is going to have all the characteristics of a common, road-legal city e-scooter, while for testing purposes, braking even at higher speeds can be tested. The motor on the rear has a round and flat housing, very useful for the mounting of a wheel-speed slotted disc on the rear (more in Section 5.6).

The accumulator is a lithium-ion battery pack, with 48 V and 10.4 Ah (486.72 Wh), ensuring a decent range. It sits as usual under the deck and can be easily accessed by removing the cover of the latter. It is connected and managed by a brushless DC motor controller, rated for up to 10 A, and with a cutoff voltage of 40 V. Most of the data from the controller can be accessed by the driver on the dashboard on the handlebar or on the Bluetooth-connected app. Very useful for future tests are the four different speed modes, restricting the speed to 6, 15, 20, or 25 km/h, meaning these speeds can be easily maintained consistently for a longer period if desired. Alternatively, the scooter offers a cruise control option, which could also prove useful in the future for the same reasons.

5.1.2 Overall design

With the brake assist system conceptualized and an e-scooter chosen, a general design for the complete vehicle had to be developed. The different macro-functionalities that the brake assist system should offer were analyzed and identified. Basically, for the brake system to work, an electric signal proportional to the driver's input has to be created. Then, together with the data about the current riding conditions, it is processed and the two brakes are actuated accordingly. In more precise terms, the main functions identified are:

- Measure the rider input and ensure adequate braking ergonomics.
- Measure the current rider position and mass.
- Measure the external factors required for the braking, such as friction coefficient, wheel speed, vehicle speed and acceleration.
- Collect this data, process it according to the chosen braking strategy and convert it into control signals for the brake actuators.
- Build up braking pressure in the system and actuate each brake according to the requested brake force magnitude and distribution.

For each of these functions, a mechanism or device has to be developed or acquired. A graphic representation of the expected packaging and size of these components can be seen in Figure 5.2. The placement of the components was also planned throughout, with the shown configuration that optimizes maintenance, wiring, and tries to minimize the impact on the e-scooter's handling. In the following sections, all of these components will be discussed, showing their requirements first and then explaining how their functionalities were achieved and implemented.

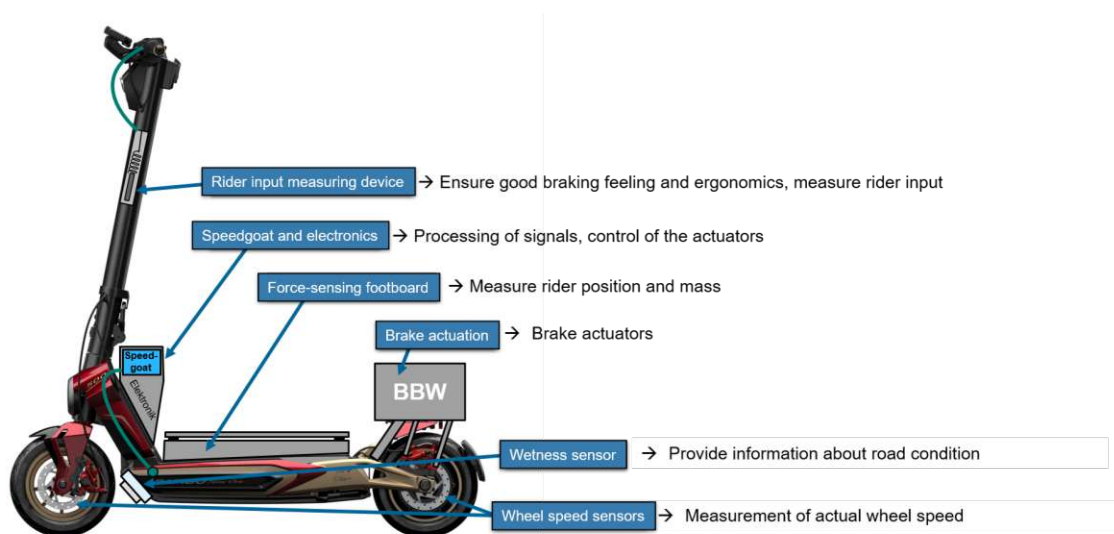


Figure 5.2: The planned vehicle packaging and functionality of each component

5.2 Rider input measuring device

Already during the initial development phase, one requirement was clearly stated: the braking system should be suitable for a wide range of riders. Keeping this in mind, ensuring a natural and instinctive braking feeling was one of the main requirements of this component.

As previously mentioned, this is a distinctive feature of brake-by-wire systems. Unlike common hydraulic or mechanical brake systems where the driver must apply the necessary brake force to stop the vehicle, in brake-by-wire systems, the system is capable of converting different force inputs – for example from a strong and a weak rider – into the same brake force, thanks to the lack of a direct mechanical connection. However, there is a drawback: the brake actuation feeling will be different from what we are all accustomed to with bicycles. The system does not naturally provide a haptic feedback or response, thus removing a valuable piece of information about the braking manoeuvre from the rider.

The first phase of the design consisted of choosing the actuation method and its packaging to maximize comfort and efficiency. Based on research [56], it was clear that positioning the single brake lever on the left side of the handlebar was the best choice. Since the classic thumb throttle is placed on the right in the current vehicle, this arrangement ensures each hand only one task: either pushing the throttle or pulling the brakes. This setup helps to limit the risk of overwhelming an inexperienced driver. The original mechanical brake lever blade mechanism was kept on purpose. This was done to ensure a more natural and familiar application of the brake, as we are all accustomed to it from riding bikes and bicycles. This setup is particularly useful in sudden danger situations, where a rider's instinctive reaction is to immediately grip the lever and squeeze it. This intuitive response would not apply, for example, to a rotational potentiometer like the one used for the throttle.

After ensuring the maximum possible ergonomic advantages with this configuration, the brake feeling had to be addressed. With the original mechanical brake lever still intact, the method chosen for measuring the lever blade travel was the measurement of the movement of the cable itself. This allowed for flexible positioning of the measuring device, utilizing the original bowden cable to guide the steel cable to the optimal position. A rendering of the final design can be seen in Figure 5.3 and the augmented reality 3D Model can be viewed with the QR code in 6.1.

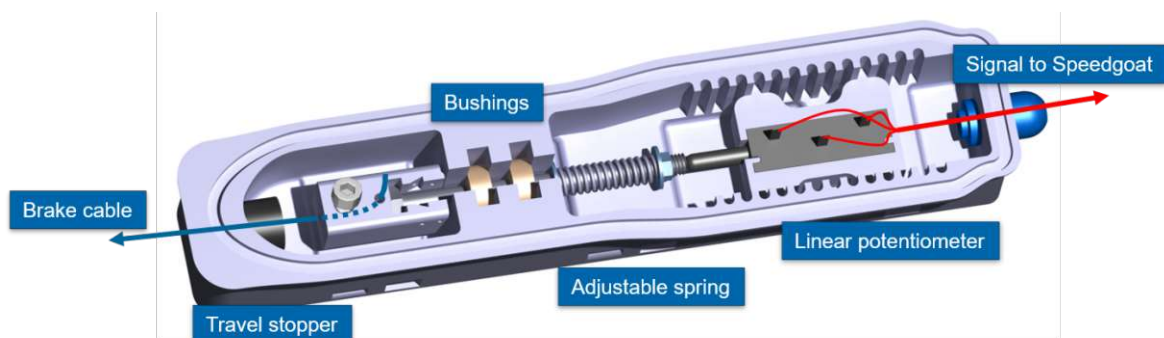


Figure 5.3: Components of the rider input measuring device

The cable pulled by the rider is attached to a 3D-printed extension of a long bolt (DIN 931 M6x100), which slides inside two pillow block bearings². The cable is pressed and held in position by a small bolt that also allows easy adjustment of the cable length. Behind the two bearings, a compression spring is placed over the bolt and squeezed into position by the casing's walls and a nut, whose purpose is to adjust the spring's pre-compression. The movement of the bolt is now purely linear because of the bushings, and thanks to the spring, it will follow the cable's movement in both directions. With this mechanism, a linear potentiometer³ can be used to measure the brake lever movement. To choose an appropriate potentiometer, the travel had to be estimated first, settling between 15 mm and 25 mm for the used model, depending on the rider's preferences. It was important to ensure that the chosen model's mechanical travel range was as close as possible to the real one to achieve the highest possible resolution. The chosen model had exactly this feature⁴, combined with a compact size and an internal compression spring to ensure steady contact with the moving bolt, proving the choice appropriate. A useful design choice was the use of 3D printing⁵. This allowed for a geometrically complex construction to fit as many features as possible into this relatively small part.

The chosen design stands out because of its significant tuning potential, allowing for different force–stroke configurations to modify the brake feel and behaviour:

1. **Spring:** The spring and bolt can be changed, with a range of the latter between 80 and 100 mm, which requires the disassembly of the whole mechanism. When changing the length of springs or bolts, the linear potentiometer can also be moved from one slot to another to provide some reserve movement of the mechanical travel, reducing the risk of damage.
2. **Spring pre-compression:** By turning the nut at the end of the bolt, the pre-compression of the spring can be adjusted, making it possible to tune it directly with a wrench. This change doesn't affect the movement or travel of the bolt, only the force required for the movement of the lever.
3. **Travel-stop:** There is the possibility and space to insert different travel stops between the bolt head and the point where the cable enters the box. Different thicknesses can be used, and the material can be tuned to provide the driver with a distinct and recognizable feeling when reaching the end of the travel and requesting maximum deceleration from the brake system. The travel stop is positioned in the front part of the casing on purpose, to make this part the only heavily stressed region of the construction, allowing the rest of the housing to be slimmer and reducing the risk of mechanical failures. Only this front part of the casing is made thicker and stronger, as the entire cable force, which is over 300 N in emergency cases according to [50], compresses this region.

²Igus igubal® pillow block bearing ESTM-06-SL, see datasheet in the appendix

³Model: Variohm KTP-10-L, see datasheet in the appendix

⁴Tests revealed an output voltage range between 0.3 and 3 V with a 5 V supply voltage over a lever blade travel of 17 mm

⁵Material: Zortrax Z-Ultrat, an ABS plastic blend, see datasheet in the appendix

4. **Bowden cable adjuster:** As usual for cable brakes, there is the possibility to elongate or shorten the bowden cable with adjustable hollow nuts at both ends, usually meant to compensate for the wear of brake pads. This feature was, of course, kept to fine-tune the travel without needing to disassemble or even open the lid.

5.3 Brake-by-wire system

The heart of the project is, of course, the braking system. The way it was conceptualized and sized has already been discussed in Chapters 3 and 4. This part deals with the concrete realization of the final prototype, addressing the practical task of finding or manufacturing the necessary and suitable components to put the developed theoretical working principles into practice. The first major task was to find the optimal way of building up the clamping force on the disc brakes in the system starting from the rotational movement of the stepper motor, chosen to actuate the brakes (see Section 3.5 for more details). The ideal system is required to have the following features:

- **Performance:** Performance requirements were drafted from the vehicle dynamics models (see Chapter 3) and from literature. For example, Maier [50] explains that the actuation speed of common bicycle brake lever blades in case of emergency braking occurs with a speed of $v = 400 \text{ mm/s}$, corresponding to 69 mm/s for the actuated brake piston, resulting in pressure rising rates of $\dot{p} = 1000 \text{ bar/s}$.
- **Compact size:** Even though the chosen e-scooter offers more room than usual to place components, the space is still limited, and rideability and handling performance need to be kept as close as possible to the original.
- **Reliability:** The system has to work reliably and consistently to ensure steady performance for the prototype use cases.
- **Feasibility:** At this stage of the development process, the availability of the components and their capabilities must be ultimately confirmed. If not, the parts must be producible using the available in-house manufacturing methods.

With these requirements, three ways of building up the pressures were taken into consideration, as shown in Figure 5.4. The actuation system is to be put in the brake-by-wire box located on the rear of the e-scooter as shown in Figure 5.2.

The first method considered was to maintain the usual brake lever–brake caliper configuration unchanged, remove it from the handlebar and place it into the appropriate actuation box. Inside the box, a **winch mechanism** would pull the brake lever blade with a cable to operate the brakes the same way as a rider would manually do. However, this concept has the main issue of combining the already mentioned reliability and elasticity problems of mechanical cable systems, essentially nullifying the advantages of using a hydraulic brake system.

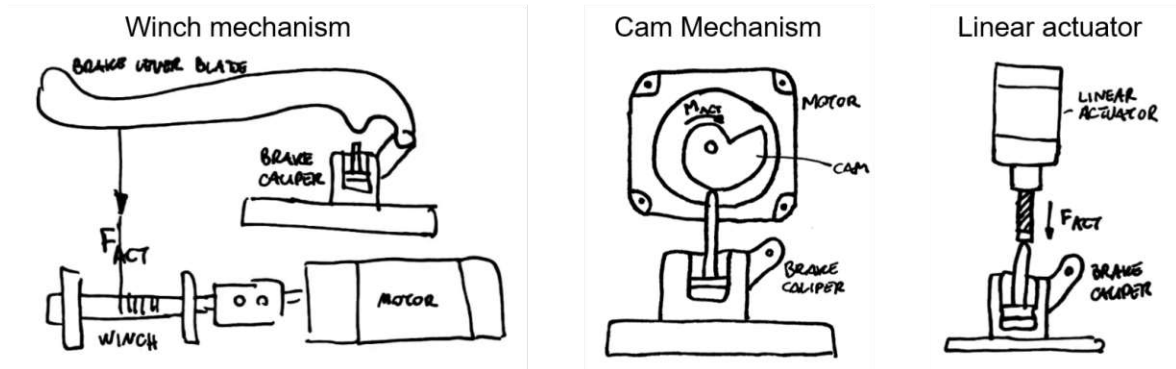


Figure 5.4: Three evaluated ways of converting the rotational movement of the motor in pressure increase in the hydraulic braking system

Additionally, the considerable size of this solution is not ideal, as it has to be repeated twice, once for the front and once for the rear.

An interesting alternative would be to use a **cam mechanism** to push the brake piston. This solution would not require the use of the lever blade, resulting in much more compact packaging. The use of a cam with a variable and customized pressure angle and size would allow specialized speed/force profiles. For example, it could increase the speed during the air gap overcoming and then increase the leverage for better force resolution when higher pressures are needed. This additional adjustability would naturally enhance performance. The cam could either be machined out of metal or 3D printed using a wear-resistant and low-friction plastic material. However, an issue identified with this design was the difficulty in synchronizing the cam profile with the movement of the piston. As mentioned in Section 2.3, the non-linearity between brake caliper position and pressure inside the brake system is challenging to model. This makes it difficult to ensure the same actuation profile under different circumstances, such as brake pad wear, friction in the system, or fluctuations in brake fluid temperature.

The last and final solution was identified as the simplest of the systems. Removing the brake lever blade for a compact design and simplifying the actuation mechanism as much as possible, a suitable solution was found in a **linear actuator** directly pushing the brake piston. This considerably simplifies the design, but it can only work properly with appropriate components that allow the realization of the very unusual brake system behaviour, as mentioned in Section 3.5.

After thorough research, the solution was identified as a stepper motor in a captive linear actuator configuration, combined with a controller capable of running the motor in torque-control mode (or force-control mode in our case)⁶. The force-control mode, as mentioned earlier, was crucial to have at disposal as it allows bypassing the common issue of modeling the uncertain relationship between piston position and brake pressure by directly setting a

⁶ Actuator model: Nanotec LGA561S20-B-TSGA-019, controller model: Nanotec CL4-E-1-12-5VDI, see datasheets in the appendix



Figure 5.5: The Magura MT4 Model with the accessible brake piston head.

force acting on the system, regardless of the current conditions. To gain more information about the behaviour of the designed system, brake pressure sensors on both the front and rear braking lines were added.

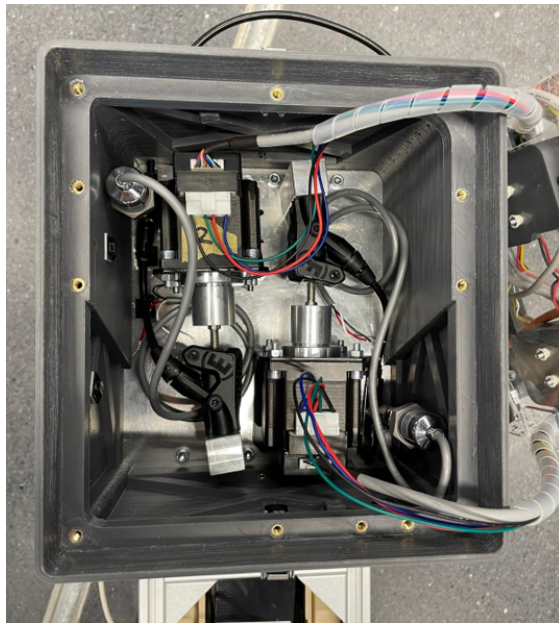
The linear movement of the actuator is achieved with a lead screw, selected with a very high pitch to enable high speeds (up to 100 mm/s) while overcoming the air gap and ensuring no self-locking, allowing for precise pressure reductions when operated in force-control mode. With this low reduction ratio, a high-torque motor had to be chosen to ensure that the maximum required pressure of 42 bar (estimated in Section 3.2) could be achieved. With the final model, forces up to 476 bar can be exerted, corresponding to a satisfactory pressure of 56 bar in the braking system.

As for the brake caliper, the ideal model was identified as the *Magura MT4*, a popular MTB hydraulic brake model. In addition to the renowned quality and reliability of the product, a very useful feature was found in the removable brake lever blade, originally meant to allow for easy switching and customization of the lever itself. By removing the lever blade, the head of the actuation brake piston is revealed and easily accessible, allowing the tip of the linear actuator to directly push it without the need for any special connection mechanism (see Figure 5.5). Additionally, the *flip-flop design* of the Magura MT brakes, which allows for the use of the brake caliper regardless of its orientation, provided considerable flexibility for the packaging task.

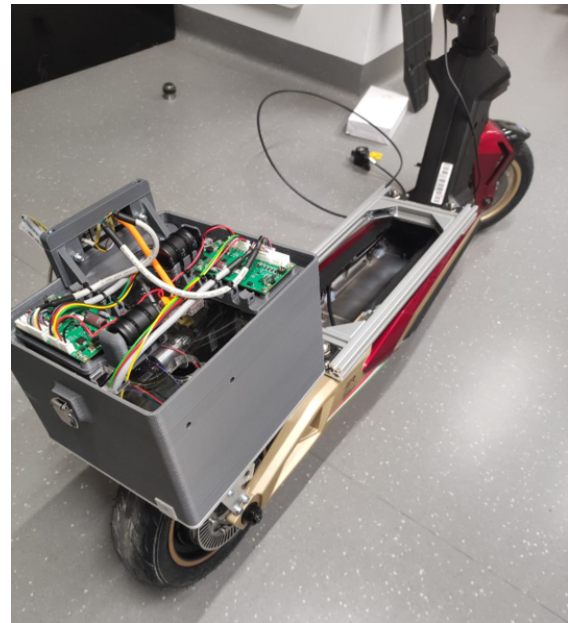
The position and configuration of this system were decided as shown in Figure 5.6 or in the 3D model accessible from 6.1. The first thing to consider was ensuring that the brake calipers with the compensating reservoir were placed higher than the brakes themselves.

For secure and stable assembly, the original mounting points of the scooter's mudguard and license plate holder have been utilized, onto which a structure of aluminium profiles serves as a solid anchoring base. On this structure, the housing base, a 5mm aluminium plate, can be easily mounted, onto which milled brake caliper mounts and linear actuators are securely attached, see Figure 5.6a. The orientation of the actuator-brake caliper combination was

chosen to use the least amount of room while providing enough space for the brake pressure to be included in the same housing. On the aluminium base plate, the housing walls are bolted and made removable to facilitate access and maintenance to the actuators. These walls are 3D printed⁷ and specifically strengthened in the rear right part, as it is planned to mount a relatively bulky and heavy non-contact optical sensor⁸ on that side at some point during the testing phases. This way, quick and clean assembly of this sensor is possible, with no need for additional strengthening structures to ensure a stable mounting point. A thick (8 mm), transparent, laser-cut acrylic glass plate tops the walls with different purposes, see Figure 5.6b. First, being securely bolted to the walls, it adds further stability to the box. Secondly, it allows observation of the movement of the actuators below, and lastly, it offers easily accessible room for the motor controllers and the wiring. To keep the wiring tidy and facilitate maintenance, the placement and mounting of all components were carefully studied, for example, by including all of each of the controllers' accessories into a single 3D printed housing or using *Wago* splicing connectors for all cables needing to be often replaced or disconnected. Since testing in wet conditions is going to be an important part of future research, a lid and cable glands for all cables and braking lines were used to fully enclose and protect all mentioned components from external agents.



(a) *Magura MT4* brake calipers and Nanotec actuators mountings and orientation



(b) Upper part of the brake-by-wire system with the protective lid removed

Figure 5.6: The assembled brake-by-wire system. Wiring and controllers are on top, actuators and brake calipers are under the acrylic glass. The optical sensor mounts are on the right side of the box, while the cable glands are on the left.

⁷As with the housing of the rider input measuring device, the material used was the ABS plastic blend Zortrax Z-Ultrat

⁸Model: Kistler Correxit S-Motion

5.4 Force-sensing footboard

The key difference between e-scooters and other two-wheeled vehicles such as motorcycles or bicycles is the variable longitudinal position of the rider. The relevance and impact of this quantity on the optimal brake balance have been thoroughly analyzed in Chapter 3, with the clear conclusion that knowledge about the longitudinal centre of gravity position of the vehicle–rider system is crucial.

This quantity determines the best braking strategy and there are different ways to determine it. The theoretically simplest and most direct way is to place some force-sensing mechanism inside the wheel hubs, measuring the vertical tyre forces directly. However, this poses some practical issues, with very limited space available on this kind of vehicle and the need to probably interfere with the bearings and axles.

A mathematical alternative to using sensors for direct measurements is to develop a rider mass and position estimator. As shown, for example, in the work of Leoni et al. [43], an accurate real-time estimation of an e-scooter rider’s mass is possible and can be accomplished without the need for special hardware. The mass can be estimated from the driving power of the vehicle and its current acceleration. The first is already measured by most motor controllers and is often also displayed on dashboards, while the second can be simply determined with an IMU (Inertial Measurement Unit), which is already part of the e-scooter testing equipment. In addition to the mass, the rider centre of gravity position must be simultaneously estimated. This is a tricky but possible task, as shown in the work of Vahidi et al. [45]. The main challenge to overcome here is the fact that the changing rate of the two quantities is very different, with the mass remaining constant throughout the ride and the rider position possibly changing within braking manoeuvre. It was decided that this mathematical method may be a later solution in this project.

Until that point, a force-sensing footboard placed over the original deck is used. This system can be used to directly measure the rider’s real-time longitudinal centre of gravity position in the first place, but also for validation once the mathematical method explained above will be introduced. The basic idea is to place four force-measuring sensors under the four edges of a stiff plate to sense the weight distribution of the rider under each corner. The total rider mass will be computed from the sum of the four measured forces, while the position along the board will be proportional to the ratio between the two front and two rear sensed values. More details about the computation method can be found in Section 3.4.

To ensure reliable and realistic results, a few precautions have to be taken. First, the board construction has to be as low as possible to minimize the deviation from the original system. Second, it’s necessary to ensure that the sensors beneath the four legs only sense the vertical load. To achieve this, movements in planar and vertical directions have to be decoupled, allowing only the latter. This means guiding the four legs vertically with a mechanism capable of absorbing longitudinal and transversal forces. This should ensure a sturdy and stable mounting while allowing near-frictionless vertical movement to minimize interference

with the vertical loads. The footboard should also include anti-lift protection to stop the vertical movement of the board at some point. Lastly, no structural modifications to the vehicle should be made, and easy disassembly should be possible.

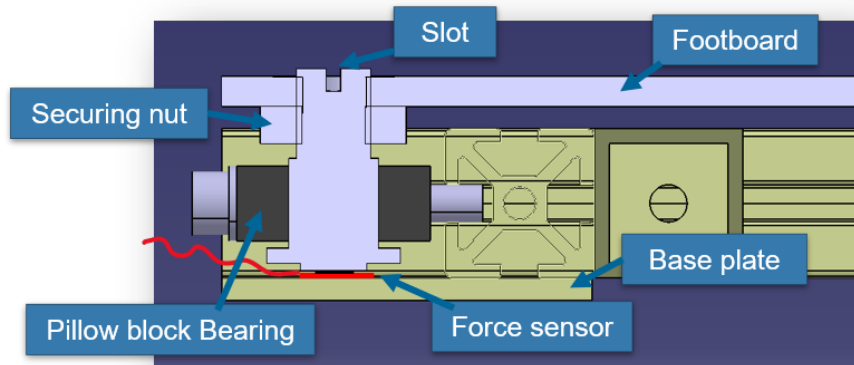


Figure 5.7: Section of one of the force-sensing footboard leg construction

The developed design that fulfils all of these requirements is shown in Figures 5.7 and 5.8. The mechanism's base is a rectangular frame of aluminium profiles mounted on spacer blocks at the four attachment points of the original deck. The thickness of these three milled blocks (one for the front and two for the rear) is chosen such that the structure is in a horizontal position. This is necessary since the original deck is slightly inclined forward. It wouldn't strictly be necessary for the force-measuring footboard to be horizontal, as the incline could be taken into consideration in the computation, but for simplification, this design choice was made. By inserting thin washers under the anchoring points, it's also possible to fine-tune the height for perfect levelling. As shown in Figure 5.7, under the front and rear frame ends, two plates are mounted, which serve as support bases for the four legs of the footboard and on which the four force sensors⁹ are fixed. These thin-film sensors (thickness: 0.2 mm), suitable for a vast range of applications, are a key component to keep the height of the whole construction as low as possible. Right at these four corners and over the sensors, plastic pillow block bearings¹⁰ are mounted, tasked with vertically guiding the plate. They are made of a plastic material¹¹ with high wear resistance and low friction characteristics, making them very suitable for the purpose at hand. Additionally, their spherical bearing automatically compensates for small alignment errors. The legs are custom-turned steel components with a large heel on the bottom to prevent excessive lifting and a fine thread on the opposite part. These are then screwed directly into the footboard itself (which has the corresponding thread in the four corners) so that the length of all four legs can be manually adjusted by turning them into the board. The basic idea is to be able to level the construction when removed from the scooter, and once the length of each leg has been chosen, it can be secured with an

⁹Sensor model: Tekscan A302, see datasheet in the appendix

¹⁰Model: igubal® pillow block bearings ESTM-12, see datasheet in the appendix

¹¹material: iglide® J

underlying lock nut. However, if needed, the milled slot on top of each leg allows for height adjustments even with the system mounted.

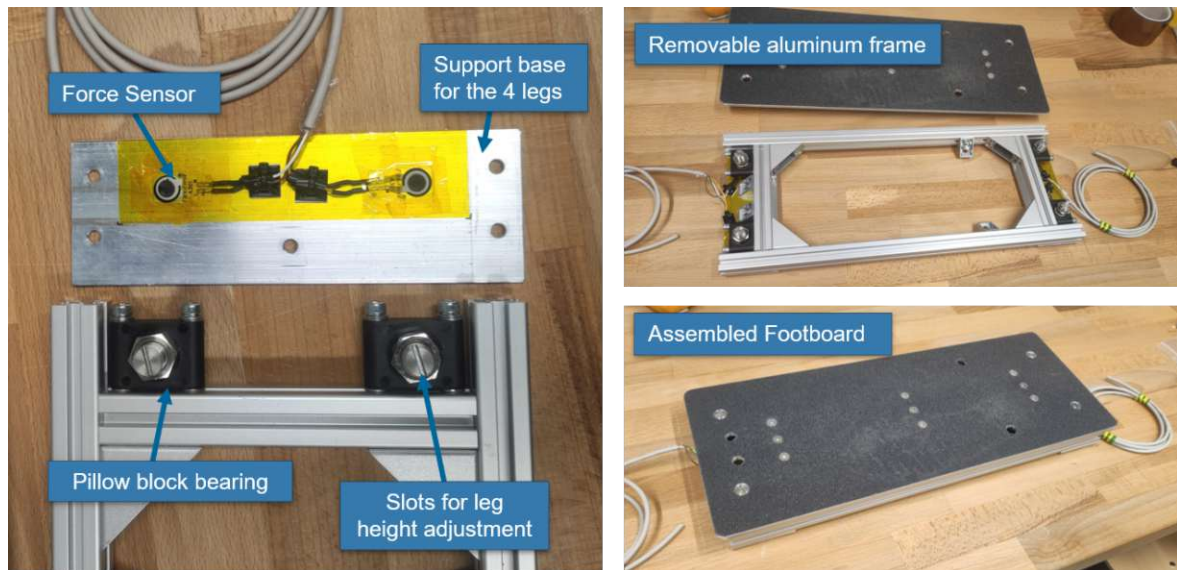


Figure 5.8: The final force-sensing footboard construction

5.5 Electronics and further sensors

To efficiently and realistically operate the brake system with a suitable strategy, an electronic control unit capable of collecting and processing extensive data is essential.

Some of the collected data has already been mentioned and explained, such as the rider's brake input or the rider's weight and position from the force-sensing footboard. Additionally, brake fluid pressure is measured directly after the brake calipers, providing useful information about the current status of the brake system. Furthermore, some other sensors are used to determine riding conditions. Similar to older e-scooters from TU Wien, a GPS sensor and an IMU are positioned next to the control unit.

The control strategies developed by Matthias Riedl [16] need to be run on this unit to derive optimal braking forces and their distribution in real-time. For this purpose, a Speedgoat Unit, a real-time target machine is utilized. This unit allows the direct implementation of self-developed MATLAB and Simulink models onboard, providing the necessary input signals for the actuators. Before being processed by the Speedgoat Unit, signals from the sensors placed on the vehicle (analogue, digital, and CAN) are collected and filtered by a separate module. This module features a custom-developed PCB to support the Speedgoat Unit, containing an STM32 microcontroller for the pre-processing of the data and a DC-DC converter for power supply.

These two components are integrated into a single modular unit designed to be easily detachable from the vehicle, facilitating their use in other projects. Therefore, they are planned to be separately mounted on the front part of the vehicle, also ensuring homogeneous

weight distribution of the testing equipment.

5.6 Road friction determination and wheel speed measuring

A critical variable to know before initiating a braking manoeuvre is, of course, the road grip. Unfortunately, this quantity cannot be measured directly, so alternative methods of estimation must be utilized. One approach is the implementation of a wetness sensor, typically positioned behind a vehicle's wheel. This sensor detects water splashes raised by the tyre to determine if the road surface is wet or dry. While not providing the exact friction coefficient, it still offers valuable information to adjust the range of the expected grip.

A potentially more precise approach is to determine the current road grip relying on calculating the actual wheel slip during acceleration or deceleration manoeuvres. Assuming the knowledge of the actual tyre forces and the use of an accurate tyre model, an estimation of the friction coefficient between the tyre and the road surface can be achieved during these driving phases.

To derive wheel slip, there are two quantities to be measured: the translational velocity of the wheels (obtainable with the Correvit optical sensor or the GPS) and the actual rotational speed of the wheels. To determine the latter, Hall effect sensors¹² were chosen and implemented on both the front and rear wheel. These sensors react to changes in the magnetic field created by a rotating metal slotted disc and are commonly used for this purpose.

Designing these discs is a delicate task because it determines the resolution and reliability of the measurement. There are several aspects that must be considered before choosing the size of the disc and the width and number of slots. Regarding the diameter of the disc, it is limited by the e-scooter's wheel geometry. Especially the rear wheel, which contains the motor, has a flat motor cap on the right side, allowing easy mounting of such a disc. The disc cannot be larger than this housing because the tyre inflation valve must still be easily accessible. For this reason, the maximum diameter on the outside was set to 120 mm. This only applies to the rear wheel, but for simplicity and maintenance reasons, both front and rear discs were designed equally.

The dimensions and number of slots had to be chosen to maximize the resolution. This means having as many slots as possible (making them very thin). Two limits needed consideration: the maximum sampling frequency of the STM32 microchip used for this task, which is 2 kHz, and the minimum required width of the gaps and teeth by the manufacturer, set at 2 mm. The initial design featured 64 slots, each with an average width of 2 mm. If considering only the passing of one tooth flank, this results in a frequency of approximately 850 Hz at the maximal predicted speed of 38 km/h. Taking the Nyquist frequency into account to avoid aliasing effects, the sampling frequency of the utilized microchip is confirmed to be high enough to reliably measure even the highest expected speeds, given that it is larger than the crucial factor of 2.

¹²Model: Variomh EURO-WS-M10, see datasheet in the appendix

However, during the laser-cutting process, overheating issues were encountered. As a result, they had to be redesigned with slightly wider slots to allow for better heat dissipation and cleaner cuts. This adjustment resulted in a small loss of resolution, as the number of slots had to be reduced from 64 to 54.

To ensure that these discs lay on a flat surface and to avoid disturbance from the metallic parts of the wheels, laser-cut acrylic glass discs were used as spacers and mounting surfaces. The rear plastic disc was glued to the flat motor cap, while the front one was clamped to the wheel spokes with custom-designed 3D-printed counterparts. Threaded inserts were melted into these acrylic glass spacers, allowing the steel discs to be easily removed or centred. Since the left side of the front wheel, which was once free, is now covered with these discs, an inflating valve extension had to be mounted to allow easy pumping of the tyre. The sensors were held in place with an arm that allows adjustment of the position in the radial direction and the air gap between the sensors and discs.

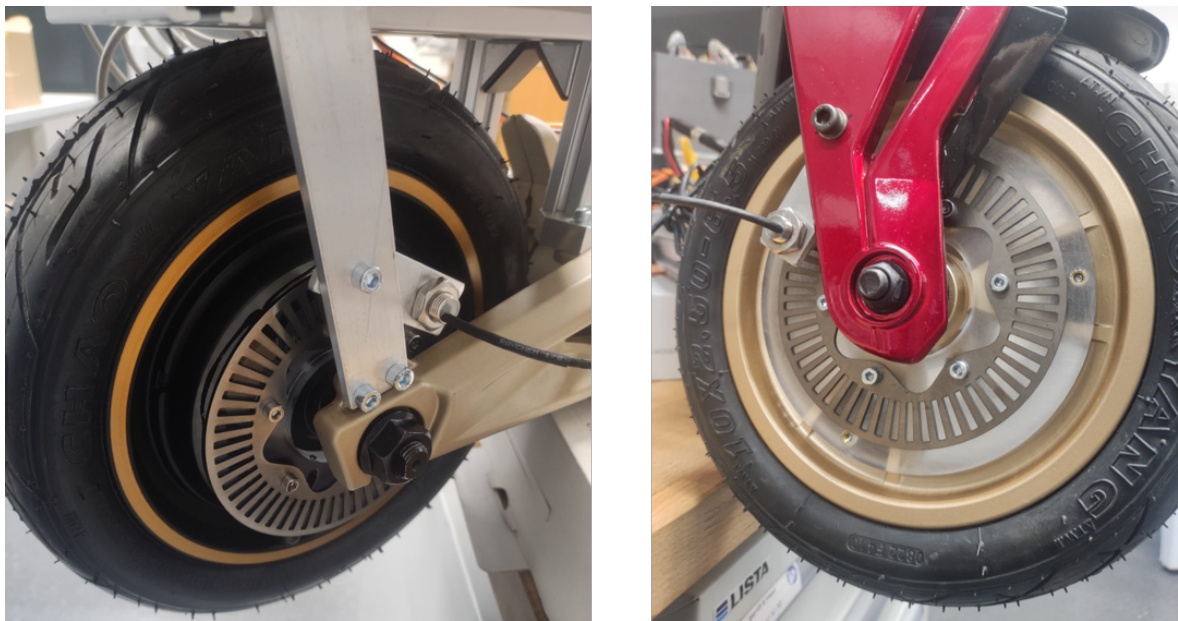


Figure 5.9: The hall effect sensors and the metallic slotted discs used to determine the actual rear and front wheel speed.

6 Conclusions

6.1 Final prototype and project continuation

The final prototype is depicted in Figure 6.1 and can also be viewed using augmented reality via the provided QR code. As illustrated, the components outlined in the previous chapter have been manufactured and implemented, with their functionality tested to a certain extent, showing positive results overall. As anticipated, the developed system is nearly ready for testing and use as a research tool. The only component not yet realized at the time of writing is the electronic control unit, primarily due to delays in component shipments.

The conducted brief tests involved the movement of a linear actuator initiated by inputs from the rider's brake lever. These tests were performed without a Simulink model; instead, a linear relationship between the brake lever's movement and the motor's was maintained for this proof of concept. The activation of the brakes was verified by examining the values returned by the brake pressure sensor. Additionally, the hall effect sensors and the force sensors under the footboard were checked, both providing values consistent with expectations.

From this stage onward, the initialization and activation phase of the scooter's components will begin, which is not further addressed in this thesis. This phase will involve calibrating all sensors and testing and validating Simulink models. Some enhancements are anticipated, as is normal when integrating various newly developed systems. As explained, systems like



Figure 6.1: Final prototype with all the implemented components

the rider input measurement system or the force-measuring footboard have been purposely designed for extensive fine-tuning, given the challenge of precisely quantifying and predicting certain behaviours. Another critical task will be determining the best-suited method for the linear actuators to accomplish braking processes. This will involve comparing and potentially combining force and position control modes until satisfactory outcomes are reached.

6.2 General considerations

Although some practical tests have already been conducted, it is still too early to draw final conclusions on most aspects. However, during the manufacturing and implementation phases, minor potential improvements for the future have already been noted. Additionally, numerous lessons have been learned during development and production, which are discussed in the following to assist future projects. Similarly, positive aspects noticed during this project will also be mentioned, along with an explanation of why they have been particularly beneficial.

Starting with the latter, the systematic and structured approach inspired by the VDI2221 standard has proven to be an effective choice. While identifying the ideal method by adapting examples and teachings from this standard was challenging and required significant effort, once established, it was very useful. It has been relatively easy to identify potentially appropriate solutions, and until the current stage, there have been no regrets about the choices made. Regarding the implementation, the careful study of many aspects influencing the designed system has allowed for very efficient and fast realization, without encountering significant issues that caused sudden changes to the original plan. The only problem that required slight revision of the plans was the previously mentioned laser cutting issues of the thin slots in the wheel speed slotted discs, which can be attributed to limited experience with this manufacturing method. Overall, I believe that this methodology was suitable for the project, especially considering the positive results, but it was also made possible by some external factors that need mentioning. For example, since most of the time (about two-thirds of the total) was spent on research and development, the time for implementation and realization was very limited. Therefore, good organization and planning for this final phase were necessary, and the manufacturing process had to be very rapid and efficient to finish in time.

However, one last positive consideration about the chosen approach was the close collaboration with the in-house manufacturing facilities. Thanks to physical proximity and repeated meetings, communication proved to be excellent and efficient, without encountering any problems of misunderstandings.

6.3 Technical considerations

Rider input measuring device

This system has already demonstrated its adaptability and the ability to experiment with various methods to enhance the braking feel. These can be tested "on road" as soon as

the electric scooter is capable of braking, ensuring a seamless integration between the input system and the braking system. However, once the correct method to provide the desired feeling is identified, an even more compact system could be aimed for. One option is to maintain the same linear configuration and to hide it within the frame next to the battery, or to convert it into a rotational measurement system and directly integrate it into the brake lever. However, even with the optimization of this component, it doesn't change the fact that the measurement is based on the movement of the lever and not on the force exerted by the rider. In future prototypes, for example, the clamping force could be directly measured by placing a dummy brake disc into a brake caliper and measuring the compression again with ultra-thin force sensors. This way, the desired braking force from the rider could be directly measured and replicated by the actuators, amplifying it with a constant value for weaker riders. Furthermore, the braking sensation, including overcoming the air gap and the increasing pressure, would be exactly the same as what we are accustomed to.

Rider mass and position determination

As previously mentioned, a system directly measuring the forces exerted on the wheel hubs would be optimal for utilizing certain braking strategies, but attempting to develop such a system could be a challenging solution. In addition to this, there may be a need to work on systems to accurately identify the height of the centre of gravity of rider as well, in order to have all available data needed to precisely calculate the overall centre of gravity. If any of these systems were proven to be functional, another possible upgrade would be to develop a system that instructs riders (especially inexperienced ones) in positioning themselves optimally on the deck. This could be achieved using visual systems (e.g. LEDs) or through vocal instructions.

Regenerative braking

A braking method that holds significant potential is the utilization of electric drive motors. It has been clearly established that they do not possess sufficient power to be used alone during heavy braking; however, this does not negate the possibility of implementing them as braking support in the future or also alone in less demanding manoeuvres. Their utilization would be advantageous since their control can be quite precise, and this braking method doesn't cause any wearing of the components involved. Particularly in the developed brake-by-wire system, integrating regenerative braking would be pretty straightforward, as the brakes are already fully managed by the onboard control unit. With appropriate control that ensures the rider a comfortable braking feeling, they could always be activated first, with the more powerful mechanical system coming to aid in case their braking power is insufficient. This approach would maximize the kinetic energy recovery, thereby enhancing the efficiency and range of the scooter. Additionally, it would enable future braking systems to be designed with smaller dimensions, given the supplementary support provided by these motors.

Bibliography

- [1] Susan Shaheen et al. “Sharing strategies: Carsharing, shared micromobility (bikesharing and scooter sharing), transportation network companies, microtransit, and other innovative mobility modes”. In: *Transportation, Land Use, and Environmental Planning*. Elsevier, Jan. 2019, pp. 237–262. DOI: 10.1016/B978-0-12-815167-9.00013-X.
- [2] Joseph Hollingsworth, Brenna Copeland, and Jeremiah X. Johnson. “Are e-scooters polluters? the environmental impacts of shared dockless electric scooters”. In: *Environmental Research Letters* 14.8 (Aug. 2019). DOI: 10.1088/1748-9326/ab2da8.
- [3] Urban Mobility. *The E-scooter trend - A popular mobility alternative*. München, 2023. URL: <https://www.iaa-mobility.com/de/newsroom/news/urban-mobility/trend-t-scooter> (visited on 12/28/2023).
- [4] Belma Turan and Tina Wakolbinger. “The Electric Scooter Collection Problem: A Case Study in the City of Vienna”. In: *Sustainability (Switzerland)* 15.13 (July 2023). DOI: 10.3390/su151310058.
- [5] Statista Research Department. *Anzahl der Unfälle mit Personenschaden bei E-Scootern in Deutschland nach Unfallfolgen in den Jahren von 2021 bis 2022*. Tech. rep. July 2023. URL: <https://de.statista.com/statistik/daten/studie/1130199/umfrage/unfaelle-mit-e-scootern-in-deutschland/> (visited on 12/29/2023).
- [6] Manuel Klinger. *Analyse der Fahrdynamik und Fahrsicherheit von E-Scootern*. Diplomarbeit. Vienna: TU Wien, 2021.
- [7] Manuel Vögl. *Analyse des Fahrverhaltens und der Fahrstabilität von e-Scootern: Simulation und Fahrversuch*. Diplomarbeit. Vienna: TU Wien, 2023.
- [8] Florian Klinger et al. “Electric Scooter Dynamics – From a Vehicle Safety Perspective”. In: *Lecture Notes in Mechanical Engineering*. Springer Science and Business Media Deutschland GmbH, 2022, pp. 1102–1112. DOI: 10.1007/978-3-031-07305-2{_}102.
- [9] Christina Garman et al. “Micro-Mobility Vehicle Dynamics and Rider Kinematics during Electric Scooter Riding”. In: *SAE Technical Papers*. Vol. 2020-April. April. SAE International, Apr. 2020. DOI: 10.4271/2020-01-0935.
- [10] Milan Paudel and Fook Fah Yap. “Front steering design guidelines formulation for e-scooters considering the influence of sitting and standing riders on self-stability and safety performance”. In: *Proceedings of the Institution of Mechanical Engineers, Part D: Journal of Automobile Engineering* 235.9 (Aug. 2021), pp. 2551–2567. DOI: 10.1177/0954407021992176.

- [11] Vittore Cossalter, Roberto Lot, and Fabiano Maggio. *On the Braking Behavior of Motorcycles*. Tech. rep. 2004, pp. 1274–1280.
- [12] Krisztian Enisz et al. “Development of a bicycle anti-lock braking system prototype”. In: *Journal of Automotive Engineering and Technologies* 3 (2014), pp. 111–118.
- [13] David Lie and Cheng Kuo Sung. *Synchronous brake analysis for a bicycle*. Tech. rep. 4. Apr. 2010, pp. 543–554. DOI: 10.1016/j.mechmachtheory.2009.11.006.
- [14] Matteo Corno et al. “On optimal motorcycle braking”. In: *Control Engineering Practice* 16.6 (June 2008), pp. 644–657. DOI: 10.1016/j.conengprac.2007.08.001.
- [15] Hanns B. Pacejka. *Tire and vehicle dynamics*. 2nd ed. Butterworth-Heinemann, Oxford, 2005.
- [16] Matthias Riedl. *Master Thesis*. Diplomarbeit. Vienna: TU Wien, 2024.
- [17] R. S. Sharp. “Limit braking of a high-performance motorcycle”. In: *Vehicle System Dynamics* 47.5 (May 2009), pp. 613–625. DOI: 10.1080/00423110802331567.
- [18] Robert Bosch GmbH. *eBike ABS: Safe braking for eBikes – Bosch eBike Systems - Bosch eBike Systems*. 2024. URL: <https://www.bosch-ebike.com/en/products/abs> (visited on 01/03/2024).
- [19] Blubrake. *Blubrake - Anti-lock braking system for e-bikes and e-cargo bikes*. 2024. URL: <https://blubrake.com/> (visited on 01/03/2024).
- [20] Chun Kuei Huang and Ming Chang Shih. “Design of a hydraulic anti-lock braking system (ABS) for a motorcycle”. In: *Journal of Mechanical Science and Technology* 24.5 (May 2010), pp. 1141–1149. DOI: 10.1007/s12206-010-0320-9.
- [21] C. Y. Lu and M. C. Shih. “Design of a hydraulic anti-lock braking modulator and an intelligent brake pressure controller for a light motorcycle”. In: *Vehicle System Dynamics* 43.3 (Mar. 2005), pp. 217–232. DOI: 10.1080/00423110412331282878.
- [22] Yuan Ting Lin et al. *Design of combined brake system for light weight scooters*. Mar. 2022. DOI: 10.1177/09544070211024093.
- [23] Oliver Maier, Martin Pfeiffer, and Jürgen Wrede. “Development of a Braking Dynamics Assistance System for Electric Bicycles: Design, Implementation, and Evaluation of Road Tests”. In: *IEEE/ASME Transactions on Mechatronics* 21.3 (June 2016), pp. 1671–1679. DOI: 10.1109/TMECH.2015.2505186.
- [24] Oliver Maier. “Modellbasierte Entwicklung eines aktiven Sicherheitssystems für elektrifizierte Fahrräder”. PhD thesis. Magdeburg: Otto-von-Guericke-Universität Magdeburg, Jan. 2018. DOI: 10.5445/KSP/1000081286.
- [25] Matteo Corno, Luca D’Avico, and Sergio M. Savaresi. “An Anti-Lock Braking System for Bicycles”. In: *2018 IEEE Conference on Control Technology and Applications, CCTA 2018*. Institute of Electrical and Electronics Engineers Inc., Oct. 2018, pp. 834–839. DOI: 10.1109/CCTA.2018.8511615.

- [26] Matteo Corno et al. *United States Patent - BRAKE ASSIST SYSTEM FOR A CYCLIST ON A BICYCLE*. Sept. 2022.
- [27] Fabio Todeschini et al. *United States Patent - ADAPTIVE BRAKE ASSIST SYSTEM FOR A CYCLIST ON A BICYCLE BY AN HAPTIC FEEDBACK*. Mar. 2022.
- [28] Rudolph Fischer. *The Blubrake ABS G2 anti-lock braking system in review - The ebike ABS for all? — E-MOUNTAINBIKE Magazine*. Nov. 2023. URL: <https://ebike-mtb.com/en/blubrake-abs-g2-anti-lock-braking-system-review/> (visited on 01/08/2024).
- [29] Ryder C. Winck, Ken Marek, and ChengShu Ngoo. *Active Anti-lock Brake System for Low Powered Vehicles Using Cable-Type Brakes*. Tech. rep. 2010.
- [30] Michael D. Machado and Vimal K. Viswanathan. “Design and Characterization of a Single Lever Bicycle Brake with Hydraulic Pressure Proportioning”. In: *Applied Sciences (Switzerland)* 13.3 (Feb. 2023). DOI: 10.3390/app13031767.
- [31] Dexiang Li et al. *Review of Brake-by-Wire System and Control Technology*. Mar. 2022. DOI: 10.3390/act11030080.
- [32] Hans-Rolf Reichel. *Elektronische Bremssysteme : vom ABS zum Brake-by-Wire*. ger. 2. Aufl. Renningen: Expert-Verl., 2003.
- [33] Fabio Todeschini et al. “Adaptive cascade control of a brake-by-wire actuator for sport motorcycles”. In: *IEEE/ASME Transactions on Mechatronics* 20.3 (June 2015), pp. 1310–1319. DOI: 10.1109/TMECH.2014.2341114.
- [34] Andrea Dardanelli, Giovanni Alli, and Sergio M. Savaresi. “Modeling and control of an electro-mechanical brake-by-wire actuator for a sport motorbike”. In: *5th IFAC Symposium on Mechatronic Systems, Cambridge, MA*. Vol. 43. 18. IFAC Secretariat, 2010, pp. 524–531. DOI: 10.3182/20100913-3-US-2015.00072.
- [35] Fabio Todeschini et al. “Adaptive position-pressure control of a brake by wire actuator for sport motorcycles”. In: *European Journal of Control* 20.2 (2014), pp. 79–86. DOI: 10.1016/j.ejcon.2013.12.003.
- [36] Fabio Todeschini et al. “Nonlinear Pressure Control for BBW Systems via Dead-Zone and Antiwindup Compensation”. In: *IEEE Transactions on Control Systems Technology* 24.4 (July 2016), pp. 1419–1431. DOI: 10.1109/TCST.2015.2483562.
- [37] Mara Tanelli, Alessandro Astolfi, and Sergio M. Savaresi. “Robust nonlinear output feedback control for brake by wire control systems”. In: *Automatica* 44.4 (Apr. 2008), pp. 1078–1087. DOI: 10.1016/j.automatica.2007.08.020.
- [38] Mara Tanelli et al. “Analysing the interaction between braking control and speed estimation: the case of two-wheeled vehicles”. In: *47th IEEE Conference on Decision and Control, Cancun, Mexico* (2008).
- [39] Chris Line, Chris Manzie, and Malcolm Good. *Control of an Electromechanical Brake for Automotive Brake-By-Wire Systems with an Adapted Motion Control Architecture*. Tech. rep. 2004, pp. 1047–1056.

- [40] Wei Han, Lu Xiong, and Zhuoping Yu. “Braking pressure control in electro-hydraulic brake system based on pressure estimation with nonlinearities and uncertainties”. In: *Mechanical Systems and Signal Processing* 131 (Sept. 2019), pp. 703–727. DOI: 10.1016/j.ymssp.2019.02.009.
- [41] Christian Junge et al. *Pressure Control of a Nonlinear System with a Linear-PMSM and a Standard Inverter*. Tech. rep. 2009, pp. 83–88.
- [42] Ralf Schwarz et al. *Clamping Force Estimation for a Brake-by-Wire Actuator*. Tech. rep. 1999, pp. 885–896.
- [43] Leoni Jessica et al. *Real Time Passenger Mass Estimation for e-scooters*. Tech. rep. 2023, pp. 1741–1746.
- [44] A. Vahidi, A. Stefanopoulou, and H. Peng. “Recursive least squares with forgetting for online estimation of vehicle mass and road grade: Theory and experiments”. In: *Vehicle System Dynamics* 43.1 (Jan. 2005), pp. 31–55. DOI: 10.1080/00423110412331290446.
- [45] Ardalan Vahidi et al. *Simultaneous Mass and Time-Varying Grade Estimation for Heavy-Duty Vehicles*. Tech. rep. 2003, pp. 4951–4956.
- [46] Matthew C. Miller et al. “Validity of a device designed to measure braking power in bicycle disc brakes”. In: *Sports Biomechanics* 17.3 (July 2018), pp. 303–313. DOI: 10.1080/14763141.2017.1338744.
- [47] Vinayak Sanjay Gaikwad and Avinash Bhausahab Jadhav. “A Review on Design of Hydraulic Disc Braking System and its Calculations for Cycle sports Bicycle”. In: *International Research Journal of Engineering and Technology* (2020), pp. 3016–3019.
- [48] Ijin Yang, Woogab Lee, and Inyong Hwang. *A Model-Based Design Analysis of Hydraulic Braking System*. Tech. rep. 2003, pp. 231–236.
- [49] Ioan Feier and Robin Redfield. “Thermal/Mechanical Measurement and Modeling of Bicycle Disc Brakes”. In: MDPI AG, Feb. 2018, p. 215. DOI: 10.3390/proceedings2060215.
- [50] Oliver Maier et al. “In-depth analysis of bicycle hydraulic disc brakes”. In: *Mechanical Systems and Signal Processing* 95 (Oct. 2017), pp. 310–323. DOI: 10.1016/j.ymssp.2017.03.044.
- [51] Robert Kühnen and Florentin Vesenbeckh. “Bremsentest-Kräfte messen”. In: *EMTB* (2020).
- [52] Robert Kühnen. “Have a Brake”. In: *BIKE* (2021).
- [53] Konrad Reif Ed. *Brakes, Brake Control and Driver Assistance Systems-Function, Regulation and Components*. Springer Fachmedien Wiesbaden, 2014. DOI: 10.1007/978-3-658-03978-3.
- [54] D K Fisher. *Brake System Component Dynamic Performance Measurement and Analysis*. Tech. rep. 1970, pp. 1157–1180.

- [55] Nicholas Famiglietti et al. “Bicycle Braking Performance Testing and Analysis”. In: *WCX™ 2020 SAE World Congress Experience* 2020-April. April (Apr. 2020). DOI: 10.4271/2020-01-0876.
- [56] Felix Wilhelm Siebert et al. “Braking bad – Ergonomic design and implications for the safe use of shared E-scooters”. In: *Safety Science* 140 (Aug. 2021), p. 105294. DOI: 10.1016/J.SSCI.2021.105294.
- [57] Verein Deutscher Ingenieure. *VDI-2221 Blatt 1 / Part 1 - Entwicklung technischer Produkte und Systeme Modell der Produktentwicklung / Design of technical products and systems Model of product design*. Tech. rep. Düsseldorf, 2019.
- [58] Verein Deutscher Ingenieure. *VDI-2221 Blatt 2 / Part 2 - Entwicklung technischer Produkte und Systeme Gestaltung individueller Produktentwicklungsprozesse / Design of technical products and systems Configuration of individual product design processes*. Tech. rep. Düsseldorf, 2019.
- [59] Ernest P. Hanavan. *A mathematical model of the human body*. Tech. rep. Wright-Patterson Air Force Base, Ohio, Aerospace Medical Research Laboratories, 1964.
- [60] Florian Klinger, Johannes Edelmann, and Manfred Plöchl. “Enhanced Braking of E-Scooters”. In: *Presentation at the Fifth Bicycle and Motorcycle Dynamics Conference, (BMD 2023)*. Delft, The Netherlands.
- [61] Maxim Bierbach et al. *Untersuchung zu Elektrokleinstfahrzeugen*. Bundesanstalt für Straßenwesen Bergisch Gladbach, 2018.
- [62] Bundesministerium für Finanzen. *RIS - Fahrradverordnung § 1*. 2017. URL: <https://www.ris.bka.gv.at/NormDokument.wxe?Abfrage=Bundesnormen&Gesetzesnummer=20001272&Artikel=&Paragraf=1&Anlage=&Uebergangsrecht=> (visited on 03/03/2024).
- [63] Bundesministerium für Klimaschutz Umwelt Energie Mobilität Innovation Technologie. *Scooter Mobilität*. Feb. 2023. URL: <https://www.oesterreich.gv.at/themen/mobilitaet/Elektro-Scooter,-Quads-und-Co/Seite.280200.html> (visited on 03/03/2024).
- [64] Nanotec. *Kategorie — Schrittmotoren — NANOTEC*. URL: <https://de.nanotec.com/knowledge-base/category/schrittmotoren> (visited on 03/04/2024).
- [65] Analog Devices. *Optimizing Stepper Motors with Microstepping — Analog Devices*. URL: <https://www.analog.com/en/lp/001/optimizing-stepper-motors-microstepping.html> (visited on 03/04/2024).
- [66] Nanotec. *Nanotec - Intelligente Antriebslösungen*. URL: <https://de.nanotec.com/> (visited on 04/19/2024).
- [67] M Corno et al. “A haptic-based, safety-oriented, braking assistance system for road bicycles”. In: *IEEE Intelligent Vehicles Symposium* (2017), pp. 1189–1194.
- [68] Rico Haase and Bosch. *Bosch E-Bike ABS – Test. Alle Infos & Test des neuen Bosch E-Bike ABS!* Aug. 2022. URL: <https://www.emtb-news.de/news/bosch-e-bike-abs-test-2023/> (visited on 02/09/2024).


Bibliography

- [69] Magura. *MAGURA Combined Braking System (CBS)*. 2023. URL: <https://magura.com/en/EUR/magura-combined-braking-system-cbs> (visited on 02/09/2024).
- [70] Michael Trzesniowski. *Rennwagentechnik - Grundlagen, Konstruktion, Komponenten, Systeme*. 1st ed. 2008, pp. 399–401.
- [71] Wilwood disc brakes. *How Does a Proportioning Valve Work? And How Do You Adjust It?* – *Wilwood Store*. Aug. 2021. URL: <https://shop.wilwood.com/blogs/news/how-does-a-proportioning-valve-work> (visited on 02/24/2024).
- [72] MV Agusta. *E-Scooter Rapido Serie Oro — e-MV Agusta E-Mobility Store – MV Agusta eMobility*. URL: <https://emvagusta.com/products/rapido-serie-oro> (visited on 03/12/2024).


A Appendix

Hall effect sensors for wheel speed computation

Wheel Speed Sensor - EURO-WS-M10


**Variohm**
Eurosensor

- Stainless Steel M10 Housing
- Non-contacting Hall-Effect technology
- NPN Open Collector output
- Long life, extreme robust
- Operating temperature range +50°C to +150°C
- Rating IP66

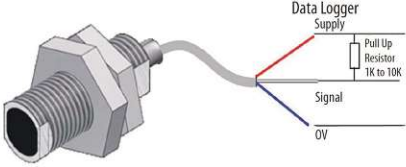


Specifications

| | |
|----------------------------|---|
| Maximum frequency | 20 kHz |
| Distance to target | 0.5 to 3 mm |
| Supply voltage | 4 to 25 V |
| Supply current | 15 mA |
| Output voltage | NPN open collector |
| Output resistance | requires pull-up resistor |
| max. voltage at the output | 25 V |
| LED indicator | Yes |
| Orientation | Side flats in the sense of rotation (see drawing) |
| Sensitive Element | Differential Hall-Effect Sensor |
| Thread | M10 x 1 mm |
| Length | 25 mm |
| Material | Stainless steel |
| Weight (without cable) | 15 g |
| Rating | IP66 |
| Vibration Test | 20 Gpp 5 |
| Shock | 500 g |
| Operating Temperature | +50 to +150°C |
| Storage Temperature | -50 to +150°C |



Dimensions



Thread: M10 x 1 mm
Length: 25 mm

Electrical connection: if the data logger has no pull up resistor, one must be added between supply (red) and signal (white) wires.

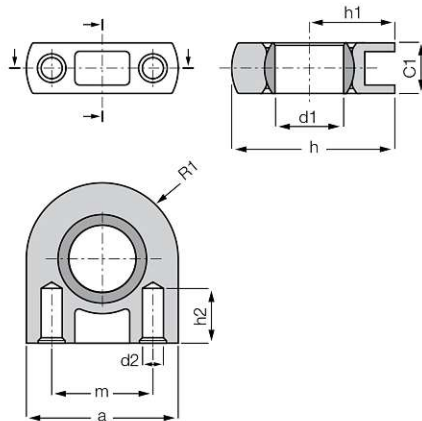
igubal® pillow block bearing used in the rider input measuring device

igubal® Pillow Block - Product range

ESTM SL - Pillow block bearing, slimline



- Lightweight
- Space saving
- Low-cost
- Predictable lifetime
- Maintenance- and lubrication free
- With M3 thread, e.g. ESTM-10-SL-M3
- For self tapping screw with outer diameter 3.5 mm
- Dimensional E series according to standard DIN ISO 12240



Order key

Type Size Version

E **ST** **M** - **05** - **SL**

| | | | | |
|----------------------|----------------------|--------|--------------|----------|
| Dimensional E series | Pillow block bearing | Metric | Inner-Ø [mm] | Slimline |
|----------------------|----------------------|--------|--------------|----------|



Material:

Housing: igumid G ▶ Page 1373
Spherical ball: iglide® J

Dimensions [mm]

| Part No. | d1 [E10] | d2 | h | h1 | h2 | a | m | C1 | R1 | Max. pivot angle |
|------------|-------------|-----|------|------|-----|------|------|-----|------|---------------------|
| ESTM-05 SL | 5.0 | 2.5 | 18.0 | 10.0 | 6.5 | 16.0 | 10.0 | 6.0 | 8.0 | 17° |
| ESTM-06 SL | 6.0 | 2.5 | 18.0 | 10.0 | 6.5 | 16.0 | 10.0 | 6.0 | 8.0 | 17° |
| ESTM-08 SL | 8.0 | 2.5 | 19.0 | 10.0 | 6.5 | 18.0 | 12.0 | 6.0 | 9.0 | 17° |
| ESTM-10 SL | 10.0 | 2.5 | 20.0 | 10.0 | 6.5 | 20.0 | 14.0 | 6.0 | 10.0 | 17° |

Technical data

| Part No. | Max. radial tensile strength | | Max. radial compressive strength | | Max. lateral strength | | Max. axial strength | | Weight [g] |
|------------|---------------------------------|-----------|-------------------------------------|-----------|--------------------------|-----------|------------------------|-----------|---------------|
| | Short term | Long term | Short term | Long term | Short term | Long term | Short term | Long term | |
| | [lbs] | [lbs] | [lbs] | [lbs] | [lbs] | [lbs] | [lbs] | [lbs] | |
| ESTM-05 SL | 337 | 169 | 315 | 157 | 202 | 101 | 34 | 17 | 1.6 |
| ESTM-06 SL | 337 | 169 | 315 | 157 | 202 | 101 | 34 | 17 | 1.7 |
| ESTM-08 SL | 360 | 180 | 315 | 157 | 214 | 107 | 22 | 11 | 1.7 |
| ESTM-10 SL | 360 | 180 | 315 | 157 | 214 | 107 | 22 | 11 | 1.9 |

3D-CAD files, prices and delivery time ▶ www.igus.com/pillow-block

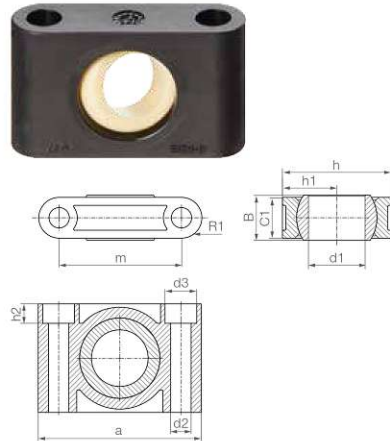
815

igubal® pillow block bearing used for the force-sensing footboard

igubal® pillow block bearings | Product range

igubal®
pillow block
bearings

Pillow block bearings: ESTM



- High radial loads
- Media-resistant
- Space-saving design, easy to fit

Order key

Type Size

E STM-08

E series **Pillow block bearing** **Metric** **Inner Ø [mm]**

Spherical ball material
Blank : iglidur® W300
J4V : iglidur® J4V
R : iglidur® R
J : iglidur® J
J4 : iglidur® J4

Material:

Housing: igumid® G ► Page 1190
Spherical ball: iglidur® W300 ► Page 175
Combination with xiros® ball bearings
► From page 1086

- Predictable service life
- Maintenance-free and lubrication-free
- Dimensional series E following DIN ISO 12240

Technical data

| Part No. | Max. radial tensile force | | Max. radial compressive strength | | Max. axial strength | | Max. tightening torque fixing holes | Weight [g] |
|------------------------|---------------------------|---------------|----------------------------------|---------------|---------------------|---------------|-------------------------------------|------------|
| | Short-term [N] | Long-term [N] | Short-term [N] | Long-term [N] | Short-term [N] | Long-term [N] | [Nm] | |
| ESTM-08 | 2,500 | 1,250 | 4,300 | 2,150 | 600 | 300 | 1.3 | 5.0 |
| ESTM-10 | 3,400 | 1,700 | 5,300 | 2,650 | 700 | 350 | 2.5 | 7.1 |
| ESTM-12 | 4,500 | 2,250 | 6,500 | 3,250 | 750 | 375 | 2.5 | 9.0 |
| ESTM-16 | 6,700 | 3,350 | 8,500 | 4,250 | 1,100 | 550 | 4.5 | 17.5 |
| ESTM-20 | 8,500 | 4,250 | 11,000 | 5,750 | 1,400 | 700 | 4.5 | 27.4 |
| ESTM-25 | 13,500 | 6,750 | 18,500 | 9,250 | 2,300 | 1,150 | 10.5 | 50.8 |
| ESTM-30 ²⁵⁾ | 10,000 | 5,000 | 16,500 | 8,250 | 2,500 | 1,250 | 10.5 | 79.7 |

²⁵⁾ Lower values loads due to different manufacturing method

Dimensions [mm]

| Part No. | d1, E10 | d2 | d3 | h | h1 | h2 | a | m | C1 | B | R1 | Max. pivot angle |
|----------|---------|------|------|----|------|------|----|----|----|----|------|------------------|
| ESTM-08 | 8 | 4.5 | – | 19 | 9.5 | – | 31 | 22 | 9 | 8 | 4.5 | 22° |
| ESTM-10 | 10 | 5.5 | – | 22 | 11.0 | – | 36 | 26 | 10 | 9 | 5.0 | 22° |
| ESTM-12 | 12 | 5.5 | – | 26 | 13.0 | – | 38 | 28 | 10 | 10 | 5.0 | 22° |
| ESTM-16 | 16 | 6.6 | 10.6 | 34 | 17.0 | 6.4 | 50 | 37 | 13 | 13 | 6.5 | 22° |
| ESTM-20 | 20 | 9.0 | 14.0 | 40 | 20.0 | 8.6 | 62 | 46 | 16 | 16 | 8.0 | 22° |
| ESTM-25 | 25 | 9.0 | 14.0 | 48 | 24.0 | 8.6 | 72 | 54 | 18 | 20 | 9.0 | 20° |
| ESTM-30 | 30 | 11.0 | 17.0 | 56 | 28.0 | 10.6 | 86 | 64 | 22 | 22 | 11.0 | 20° |

Alternative spherical ball materials ► Page 993



EN 09/2023

igus

3D CAD files, prices and delivery times online ► www.igus.eu/pillow-block 931

Linear potentiometer in the rider input measuring device

KTP Spring Return Linear Position Sensor



- Aimed at space-limited position feedback applications
- Durable design for harsh environments
- High temperature stability



Designed for a variety of space-limited feedback applications that require position feedback.. The KTP Series Linear Position Sensor is ideally suited for use where reliability in a harsh operating environment is a primary consideration.

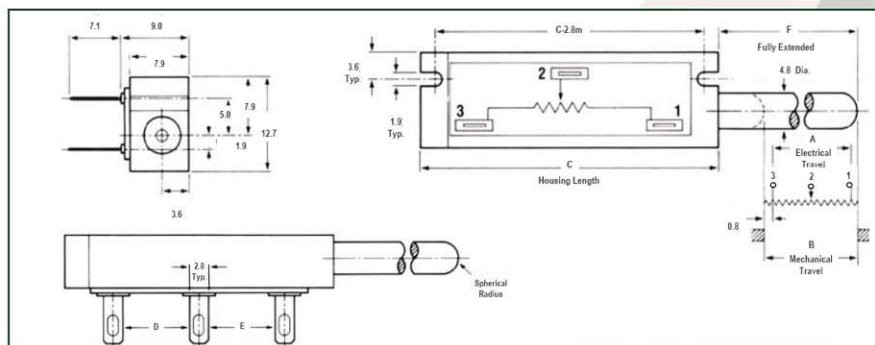
Industrial, vehicular, appliance, machine tool and robotic applications benefit from the unit's high temperature stability. The solderable terminal tabs, suitable for use with .110" (2.8mm) PDQ styled crimped wiring lugs, and durable spring-loaded plunger, make installation and operation easy.

The KTP Series is available in three standard sizes and provides excellent life at 1,000,000 full cycles (5 million dither cycles), which means high reliability in demanding installations.

Specifications

| Model | | KTP | KTP | KTP |
|---|----------|--|--------------|--------------|
| Part Number | | KTP-05-L | KTP-10-L | KTP-15-L |
| Total Electrical Travel (A) | mm | 12.7 | 25.4 | 38.1 |
| Total DC Resistance $\pm 25\%$ | Ω | 1.7K | 3.4K | 5.1K |
| Max. Voltage | V | 60 AC/DC | | |
| Linearity Over Active Electrical Travel | % | ± 2 | | |
| Best Practical Linearity (Option) | % | ± 1.0 | ± 0.5 | ± 0.35 |
| Power Rating at 70°C, | Watt | 0.25 | 0.50 | 0.75 |
| Mechanical Travel ± 0.4 (B) | mm | 14.2 | 26.9 | 39.6 |
| Housing Length ± 0.4 (C) | mm | 26.9 | 39.6 | 52.3 |
| Terminal Spacing (D) mm (E) | mm | 7.6 5.1 | 12.7 12.7 | 20.3 17.8 |
| Fully Extended Length ± 0.4 (F) | mm | 20.6 | 33.3 | 46.0 |
| Mechanical Life | - | 1,000,000 Full Cycles; 5,000,000 Dither Cycles | | |
| Stop Strength | N | 100 | | |
| Actuation Force Newtons | N | 4.0 Maximum, supplied with internal spring to return actuator to extended position | | |
| Humidity | - | 95% @ 38°C | | |
| Vibration | - | 15g, 50 to 1,000Hz, 2 hrs, each axis | | |
| Shock | g | Up to 50 | | |
| Temperature Limits | °C | -40 to +135 | | |

Dimensions & wiring



Variohm EuroSensor - Williams' Barn - Tiffeld Road - Towcester - Northants - NN12 6HP - UK
sales@variohm.com • www.variohm.com • +44 (0) 1327 351004

Subject to change without notice

KTP Spring Return Position Sensor 18/07

3D printing material

MATERIAL DATA SHEET

Z-ULTRAT

Date of issue: 01.08.2014 | Update: 13.12.2016 | Version: 1.06

Material Data Sheet: Z-ULTRAT

| Physical Properties | Metric | English | Comments |
|-------------------------|--|---|------------------------|
| Density | 1.04 g/cm ³ | 8.679 lbs/gal | ISO 1183 |
| Mold Shrinkage, Flow | 0.5 - 0.8% Thickness 3.20 mm | 0.5 - 0.8% Thickness 0.126 in | |
| Melt Flow | 11.7 g/10 min Load 3.80 kg, Temperature 230 °C | 0.0257 lb/10 min Load 8.38 lb, Temperature 446 °F | ASTM D1238 |
| | 12 g/10 min Load 5 kg, Temperature 220 °C | 0.0265 lb/10 min Load 11 lb, Temperature 428 °F | ISO 1183 |
| | 42 g/10 min Load 10 kg, Temperature 220 °C | 0.0926 lb/10 min Load 22 lb, Temperature 428 °F | |
| Melt Viscosity | 1720 1000 sec ⁻¹ , Temperature 240 °C | 1720 1000 sec ⁻¹ , Temperature 464 °F | ASTM D3825 |
| Mechanical Properties | Metric | English | Comments |
| Hardness, Rockwell R | 113 | 113 | |
| Tensile Strength, Yield | 46 MPa 5 mm/min | 6600 psi 0.2 in/min | ASTM D638 |
| | 46 MPa 50 mm/min | 6600 psi 1.96 in/min | ISO 527 |
| Tensile Strength, Break | 35 MPa 5 mm/min | 5000 psi 0.2 in/min | ASTM D638 |
| | 35 MPa 50 mm/min | 5000 psi 1.96 in/min | ISO 527 |
| Elongation at Yield | 2 % | 2 % | 5 mm/min; ASTM D638 |
| | 2.3 % | 2.3 % | 50 mm/min; ISO 527 |
| Elongation at Break | 18 % | 18 % | 5 mm/min; ASTM D638 |
| | 40 % | 40 % | 50 mm/min; ISO 527 |

www.zortrax.com | 1

MATERIAL DATA SHEET

Z-ULTRAT

| Tensile Modulus | 2.45 GPa | 355 ksi | ISO 527 |
|-------------------------------------|--|--|---------------------------|
| | 1 mm/min | 0.04 in/min | |
| | 2.48 GPa | 360 ksi | ASTM D638 |
| | 5 mm/min | 0.19 in/min | |
| Izod Impact, Notched | 80 J/m Temperature -30.0 °C | 1.4 ft-lb/in Temperature -22.0 °F | ASTM D256 |
| | 240 J/m Temperature 23.0 °C | 4.4 ft-lb/in Temperature 73.0 °F | |
| | 7 kJ/m ² 80x10x4 mm, Temp -30.0 °C | 3.33 ft-lb/in ² 3.15x0.394x0.157 in, Temperature -22.0 °F | ISO 180/1A |
| | 16 kJ/m ² 80x10x4 mm, Temp 23.0 °C | 7.61 ft-lb/in ² 3.15x0.394x0.157 in, Temperature 73.0 °F | |
| Charpy Impact, V-notch | 18 kJ/m ² 80x10x4 mm, Span 62 mm | 8.57 ft-lb/in ² 3.15x0.394x0.157 in, Span 2.44 in | ISO 179/1eA |
| Flexural Strength, Yield | 79 MPa 1.3 mm/min, 50 mm span | 11458 psi 0.05 in/min, 2 in span | ASTM D790 |
| | 70 MPa 2 mm/min | 10153 psi 0.079 in/min | ISO 178 |
| Flexural Modulus | 2.62 GPa 1.3 mm/min, 50 mm span | 380 ksi 0.05 in/min, 2 in span | ASTM D790 |
| | 2.5 GPa 2 mm/min | 363 ksi 0.079 in/min | ISO 178 |
| Instrumented Impact Total Energy | 5 J Temperature -30.0 °C | 44 in-lb Temperature -22.0 °F | ASTM D3763 |
| | 21 J Temperature 23.0 °C | 185 in-lb Temperature 73.0 °F | ASTM D3763 |
| Thermal Properties | Metric | English | Comments |
| Vicat Softening Point | 98.0 °C | 208.4 °F | Rate B/50; ASTM D 1525 |
| | 98.0 °C | 208.4 °F | Rate B/50; ISO 306 |
| | 100.0 °C | 212.0 °F | Rate B/120; ISO 306 |
| Flame Class Rating | HB Thickness 1.52 mm | HB Thickness 0.0598 in | UL94 |

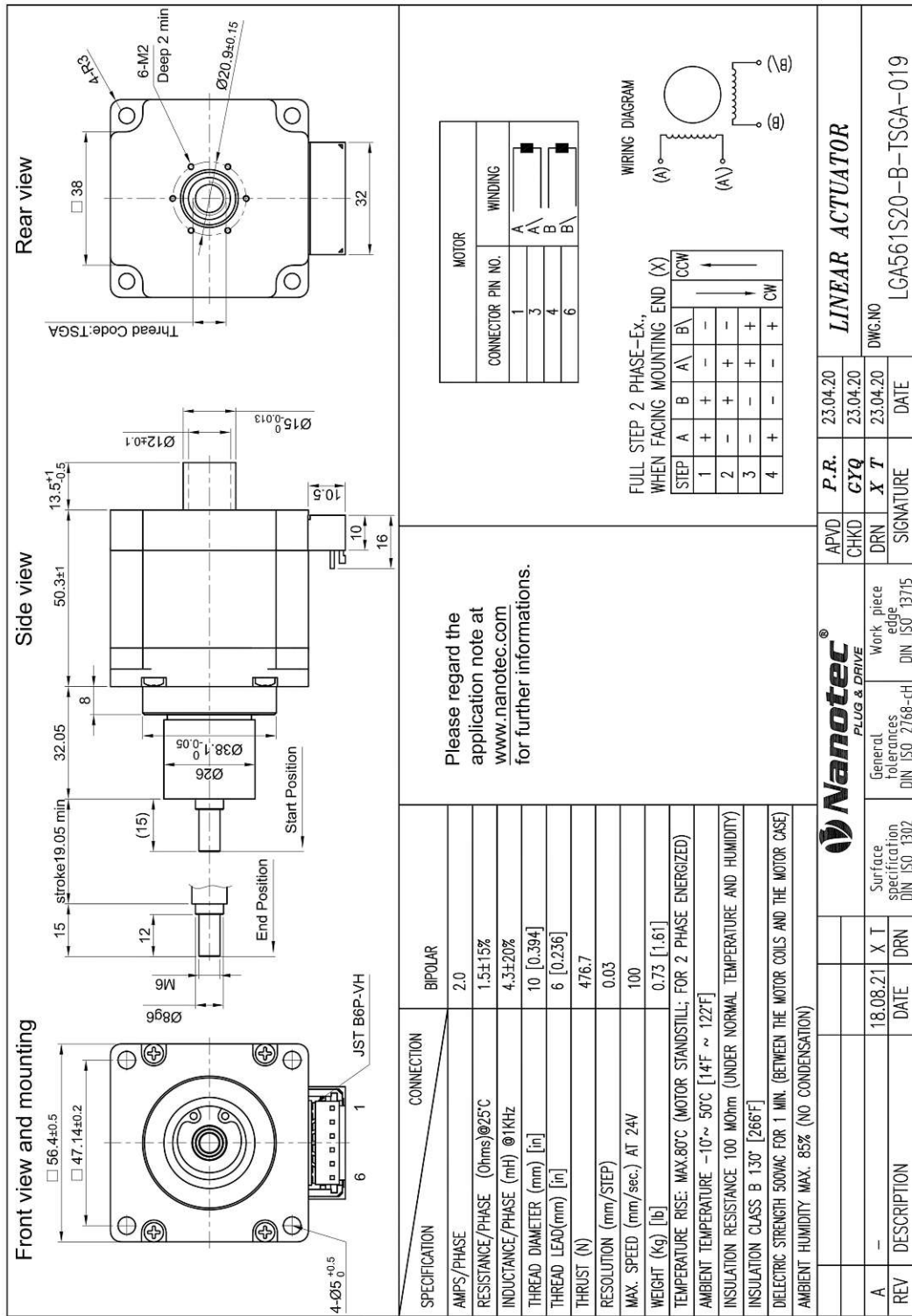
MATERIAL DATA SHEET

Z-ULTRAT

| | | | |
|---|--------------------------------------|--|--------------------------|
| Coefficient of Thermal Expansion | 8.82E-05 1/°C -40.0 °C to 40.0 °C | 4.9E-05 1/°F -40.0 °F to 104 °F | ASTM E 831; flow |
| | 8.46E-05 1/°C -40.0 °C to 40.0 °C | 4.7E-05 1/°F -40.0 °F to 104 °F | ASTM E 831; xflow |
| | 8.82E-05 1/°C -40.0 °C to 40.0 °C | 4.9E-05 1/°F -40.0 °F to 104 °F | ISO 11359-2; flow |
| | 8.46E-05 1/°C -40.0 °C to 40.0 °C | 4.7E-05 1/°F -40.0 °F to 104 °F | ISO 11359-2; xflow |
| Deflection Temperature at 0.45 MPa (66 psi) | 95 °C Thickness 3.20 mm | 203.0 °F Thickness 0.126 in | Unannealed; ASTM D648 |
| Deflection Temperature at 1.82 MPa (264 psi) | 82 °C Thickness 3.20 mm | 179.6 °F Thickness 0.126 in | Unannealed; ASTM D648 |
| Deflection Temperature at 0.45 MPa (66 psi) | 89 °C 120x10x4 mm sp=100 mm | 192.2 °F 4.72x0.394x0.157 in sp=3.937 in | ISO 75/Be |
| Deflection Temperature at 1.8 MPa (264 psi) | 76 °C 120x10x4 mm sp=100 mm | 168.8 °F 4.72x0.394x0.157 in sp=3.937 in | ISO 75/Ae |
| Relative Temperature Index, Electrical | 60 °C | 140 °F | UL 746B |
| Relative Temperature Index, Mechanical with Impact | 60 °C | 140 °F | UL 746B |
| Relative Temperature Index, Mechanical without Impact | 60 °C | 140 °F | UL 746B |

A Appendix

Linear actuator for the brakes



For the technical manual and datasheet of the controller, see: <https://de.nanotec.com/produkte/2694-cl4-e-1-12-5vdi>